UNIVERSITY OF NAPLES FEDERICO II

DOCTORATE
MOLECULAR MEDICINE AND MEDICAL BIOTECHNOLOGY

XXXI CICLO

Innovative strategies for the generation of novel human therapeutic anti-tumor and immunomodulatory antibodies

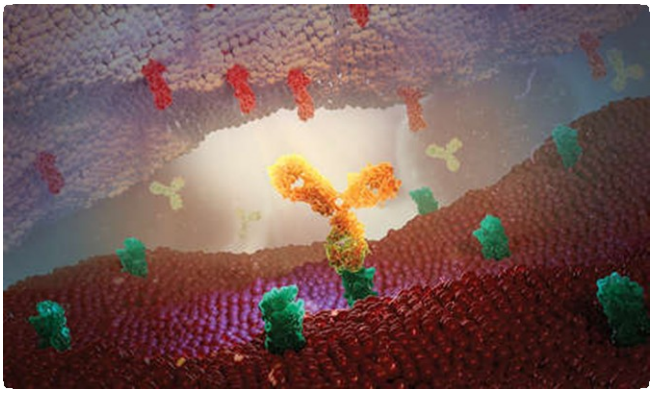

Tutor
Prof. Claudia De Lorenzo

Candidate
Margherita Passariello

COORDINATOR

Prof. Vittorio Enrico Avvedimento

Academic Year 2017/2018

ABSTRACT

Immunotherapy, based on the use of novel human mAbs endowed with antitumor or immunomodulatory activity, is an increasingly important strategy for cancer therapy. Monoclonal antibodies can be directed against Tumor Associated Antigens (TAAs), to inhibit their oncogenic function, or against Immune Checkpoints (IC), to modulate specific T cell responses against cancer. Furthermore, ongoing clinical trials in oncology are currently testing combinatorial treatments of anti-TAA and immunomodulatory antibodies.

In our laboratory novel human antitumor immunoagents have been successfully produced against the TAA ErbB2, which is a Tyrosine Kinase Receptor, overexpressed in breast cancer and several other carcinomas. In particular, a fully human single chain antibody fragment (scFv), named Erbicin, able to bind to an epitope of ErbB2 different from those recognized by the clinically validated mAbs Trastuzumab and Pertuzumab, was isolated by phage display selection on live cells. A human anti-ErbB2 “compact antibody” (100kDa) was also generated by the fusion of Erbicin with a human IgG1 Fc, which was found to efficiently inhibit ErbB2-positive tumor growth both *in vitro* and *in vivo*.

As a further progress, a trispecific antibody derivative, named Tribody, targeting three noncompeting epitopes on the extracellular domain of ErbB2 was obtained by fusing 3 binding moieties derived from Erb-hcAb, Trastuzumab and Pertuzumab, respectively. The triparatopic Tribody significantly downregulates ErbB2 and inhibits the cell growth of tumor cells, including those resistant to Trastuzumab. We show here that the multiparatope tribody combines and potentiates the therapeutic effects of the 3 different antibodies in 1 single antibody construct, thus allowing for the reduction of costs of antibody production and overcoming the limits related to monotherapy associated drug resistance.

On the other hand, we performed a massive parallel screening of phage antibody library to obtain a large repertoire of fully human

immunomodulatory antibodies against several-immune regulatory checkpoints to be used in monotherapy or in combinatorial treatments for cancer therapy. We used for the first time an innovative selection strategy on human activated lymphocytes to generate a large collection of scFvs against 10 different IC, called “Immunome Library”, from which scFvs specifically recognizing a given receptor could be pulled out by subsequent affinity selection cycles on recombinant purified proteins used as baits. By Next Generation Sequencing and bioinformatic analysis we ranked individual scFvs in each collection and identified those with the highest level of enrichment. Human IgGs from three of these collections (i.e. PD-1, PD-L1 and LAG-3) were generated and tested for their binding and biological activity. In particular, they were found to specifically bind to their targets with high affinity, to efficiently activate T cell proliferation, induce cytokine secretion and inhibit *in vivo* tumor growth. Interestingly, the novel isolated mAbs have comparable or even better binding affinity and biological activity than the clinically validated anti-PD-1 mAb Nivolumab.

SOMMARIO

L'immunoterapia, basata sull'impiego di nuovi anticorpi umani dotati di attività antitumorale o immunomodulatoria, rappresenta un'importante strategia per la terapia del cancro. Gli anticorpi monoclonali possono essere diretti contro Antigeni Associati a Tumore (TAA), allo scopo di inibire la loro funzione oncogenica, oppure contro proteine di superficie di cellule del sistema immunitario (Immune Checkpoints, IC), per modulare specifiche risposte dei linfociti T contro il cancro. Peraltro, sperimentazioni cliniche in corso nel campo dell'oncologia stanno attualmente valutando l'efficacia di trattamenti combinatoriali che includono anticorpi contro TAA e anticorpi con attività di modulazione del sistema immunitario.

Nel nostro laboratorio sono stati prodotti con successo nuovi immunoagenti umani con attività antitumorale diretti contro il Recettore Tirosina-Chinasico ErbB2, un noto Antigene Associato a Tumore, iper-espresso nel carcinoma mammario ed in diversi altri tipi di tumore. In particolare, è stato isolato, mediante la tecnologia "phage display" applicata su cellule tumorali vive, un frammento anticorpale interamente umano, chiamato Erbicin, capace di legare un epitopo del recettore ErbB2 diverso rispetto a quello riconosciuto dagli anticorpi Trastuzumab e Pertuzumab, attualmente in uso clinico. Mediante la fusione di Erbicin con il dominio Fc di un anticorpo umano con isotipo IgG1 è stato anche generato un "anticorpo compatto" umano (ErB-hcAb, 100kDa) contro il recettore ErbB2, che si è mostrato capace di inibire efficientemente, sia *in vitro* che *in vivo*, la crescita di tumori ErbB2-positivi. Come ulteriore progresso, la fusione dei 3 domini di legame derivati da Erb-hcAb, Trastuzumab e Pertuzumab, ha consentito di ottenere un derivato trispecifico, chiamato *Tribody*, che riconosce 3 epitopi non competitivi sul dominio extracellulare del recettore ErbB2. Il *Tribody* triparatopico riduce significativamente i livelli di ErbB2 ed inibisce la crescita delle cellule tumorali, incluse quelle resistenti al trattamento con Trastuzumab. In questo lavoro di tesi mostriamo che il *Tribody* multiparatopico combina e potenzia gli effetti terapeutici dei tre differenti anticorpi in un solo costrutto, avendo pertanto il vantaggio

di consentire la riduzione dei costi di produzione rispetto a quelli di 3 diversi anticorpi e di superare i problemi relativi alla resistenza ai farmaci usati in monoterapia.

Parallelamente, in questo progetto di tesi abbiamo effettuato uno *screening* massivo di un repertorio di fagi esprimenti frammenti anticorpali umani allo scopo di ottenere una collezione di anticorpi interamente umani con attività immunomodulatoria diretti contro una vasta gamma di molecole chiave regolatrici del sistema immunitario, utili per la terapia del cancro in monoterapia o in trattamenti combinatoriali. A tale scopo, abbiamo usato per la prima volta una strategia di selezione su linfociti umani attivati allo scopo di generare un'ampia collezione di frammenti anticorpali a singola catena (scFvs) diretti contro 10 differenti IC, chiamata "Immunoma", dalla quale attraverso cicli successivi di selezione su proteine ricombinanti purificate fosse possibile ottenere scFvs capaci di riconoscere specificamente ciascun recettore. Tecniche di sequenziamento di ultima generazione e analisi di bioinformatica ci hanno consentito di identificare le sequenze degli scFvs più arricchite per ciascuna selezione. Sono stati generati anticorpi umani a partire da tre di queste collezioni (i.e. PD-1, PD-L1 e LAG-3), che sono stati analizzati per la loro capacità di legame ed attività biologica. In particolare, essi sono risultati capaci di riconoscere specificamente i propri bersagli e legarli con alta affinità, di attivare efficientemente la proliferazione dei linfociti T, di indurre la secrezione delle citochine ed inibire la crescita tumorale *in vivo*. E' interessante notare che i nuovi anticorpi isolati hanno un'affinità di legame ed un'attività biologica paragonabile o anche migliore di Nivolumab, l'anticorpo in uso clinico specifico per PD-1.

INDEX

List of Figures and Tables

INTRODUCTION

1. Immunotherapy of cancer

Cancer immunotherapy is aimed at stimulating immune system against cancer and exploiting the properties of its components to specifically recognize the Tumor Associated Antigens (TAAs) and selectively attack cancer cells. Once immune cells are specifically stimulated against tumors, they provide a constant surveillance and protection against tumor relapse, due to induction of specific and long-lasting memory. Nevertheless, tumors escape from immunosurveillance by acquisition of hallmark capabilities to develop several different mechanisms, such as reduction of the expression of Major Histocompatibility Complex I (MHC I) and co-stimulatory ligands, and secretion of immunosuppressive factors **(Koebel et al. 2007; Papaioannou et al. 2016; Hanahan and Weinberg 2011).** Even though some crucial discoveries started in the 70s relative to dendritic cells, followed by the development of the first chimeric antigen receptors in 1989, the cloning of the first tumor antigen in 1991 and the successive identification of the first checkpoint molecule, named cytotoxic T lymphocyte-associated protein 4 (CTLA 4) in 1995, **(Steinman and Cohn 1973; Gross et al. 1989; Leach et al. 1996),** cancer immunotherapy has particularly evolved after 2000.

Many immunotherapeutic treatments are already in clinical practice as they have been approved by the Food and Drug Administration (FDA) for treating cancer patients (**see Table 1**) (**Galluzzi et al. 2014)**. New classes of targeted drugs are emerging and many of them are already in clinical trials.

Paradigm	Agent	Indication(s)	Year*	Proposed mechanism of action
Immunomodulatory mAbs	Ipilimumab	Melanoma	2011	Blockage of CTLA4-dependent immunological checkpoints
	Nivolumab	Melanoma	2014	Blockage of PDCD1-dependent immunological checkpoints
	Pembrolizumab	Melanoma	2014	Blockage of PDCD1-dependent immunological checkpoints
Tumor-targeting mAbs	Alemtuzumab	Chronic lymphocytic leukemia	2001	Selective recognition/opsonization of $CD52^+$ neoplastic cells
	Bevacizumab	Colorectal carcinoma Glioblastoma multiforme Cervical carcinoma Lung carcinoma Renal cell carcinoma	2004	VEGFA neutralization
	Brentuximab vedotin	Anaplastic large cell lymphoma Hodgkin's lymphoma	2011	Selective delivery of MMAE to $CD30^+$ neoplastic cells
	Blinatumumab	Acute lymphoblastic leukemia	2014	CD3- and CD19-specific BiTE
	Catumaxomab	Malignant ascites in patients with $EPCAM^+$ cancer	2009	CD3- and EPCAM-specific BiTE
	Cetuximab	Head and neck cancer Colorectal carcinoma	2004	Inhibition of EGFR signaling
	Denosumab	Breast carcinoma Prostate carcinoma Bone giant cell tumors	2011	Inhibition of RANKL signaling
	Gemtuzumab ozogamicin	Acute myeloid leukemia	2000	Selective delivery of calicheamicin to $CD33^+$ neoplastic cells
	Ibritumomab tiuxetan	Non-Hodgkin lymphoma	2002	Selective delivery of ^{90}Y or ^{111}In to $CD20^+$ neoplastic cells
	Panitumumab	Colorectal carcinoma	2006	Inhibition of EGFR signaling
	Pertuzumab	Breast carcinoma	2012	Inhibition of HER2 signaling
	Obinutuzumab	Chronic lymphocytic leukemia	2013	Selective recognition/opsonization of $CD20^+$ neoplastic cells
	Ofatumumab	Chronic lymphocytic leukemia	2009	Selective recognition/opsonization of $CD20^+$ neoplastic cells
	Ramucirumab	Gastric or gastroesophageal junction adenocarcinoma	2014	Inhibition of KDR signaling
	Rituximab	Chronic lymphocytic leukemia Non-Hodgkin lymphoma	1997	Selective recognition/opsonization of $CD20^+$ neoplastic cells
	Siltuximab	Multicentric Castleman's disease	2014	IL-6 neutralization
	Tositumomab	Non-Hodgkin lymphoma	2003	Selective recognition/opsonization of, or selective delivery of ^{90}Y or ^{111}In to, $CD20^+$ neoplastic cells
	Trastuzumab	Breast carcinoma Gastric or gastroesophageal junction adenocarcinoma	1998	Selective recognition/opsonization of, or selective delivery of mertansine to, $HER2^+$ cancer cells

Table 1. Anticancer immunotherpeutics approved by FDA and currently in clinical use (Galluzzi et al. 2014).

To date, the acquired knowledge on the mechanisms of anti-tumor immune responses and the novel technological platforms suggest possible innovative means to induce more efficient and durable responses in cancer patients.

Cancer immunotherapy is based on two main approaches: passive and active treatments (**Figure 1**) (**Papaioannou et al. 2016).**

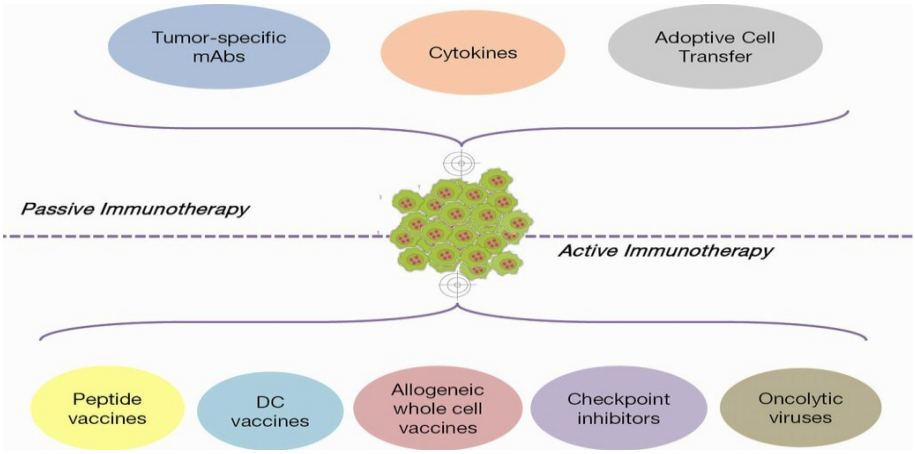

Figure 1. **Classification of active and passive cancer immunotherapy.** The passive cancer immunotherapy approach includes the tumor specific mAbs, cytokines and adoptive cell transfer. The active immunotherapy approach includes vaccines, checkpoint inhibitors and oncolytic viruses **(Papaioannou et al. 2016).**

The active immunotherapy approach involves anti-cancer vaccines (peptide, dendritic cell-based and allogeneic whole cell vaccines), as well as immune checkpoint inhibitors and oncolytic viruses. On the other hand, the best example of passive immunotherapy is represented by the treatment with monoclonal antibodies (mAbs) that have been initially used in targeted therapy against Tumor Associated Antigens **(Papaioannou et al. 2016).** Recently, many other antibodies targeting immune checkpoints have been approved by FDA for clinical use of melanoma and other cancer types **(Galluzzi et al. 2014),** due to their immunomodulatory functions, thus representing a novel approach for immunotherapy.

Furthermore, the combinations of different immunotherapy interventions are also under investigation. The combinatorial approach should be elegantly orchestrated by boosting anti-cancer responses (PUSH), on one hand, and by neutralizing negative immune regulators (PULL), on the other hand (**Figure 2**). The combination of different cancer treatment modalities (e.g., chemotherapy and checkpoint inhibitors) and the expansion of targeted drug repertoire through the discovery of new targets, new drugs and new molecules

targeting multiple molecular pathways (e.g., pan-tyrosine kinase inhibitors) are the new challenges for several research groups (**Papaioannou et al. 2016).**

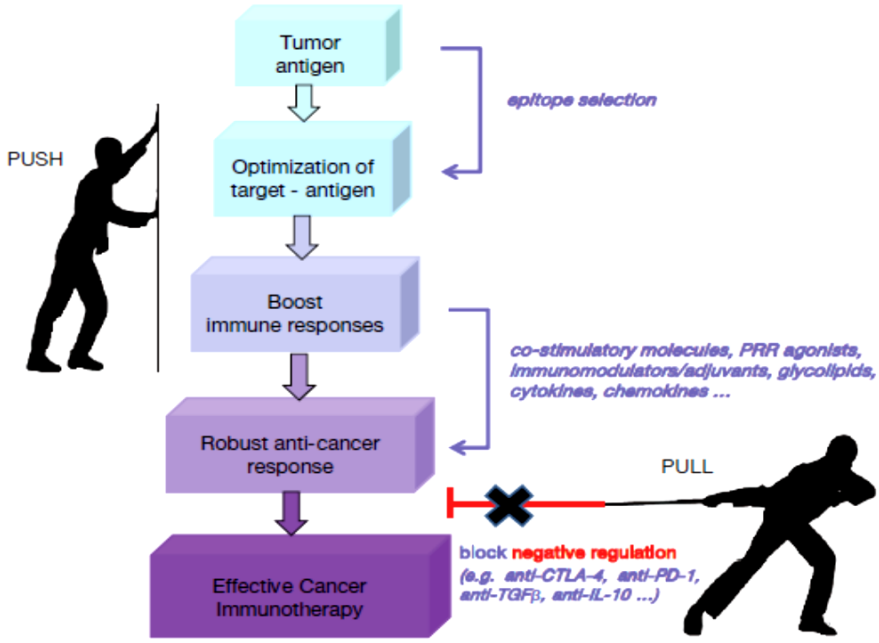

Figure 2. **The synergy between different cancer treatments.** The use of different immunotherapeutic approaches to combine the induction of immune anti-cancer responses (PUSH) with the inhibition of negative immune regulators (PULL) **(Papaioannou et al. 2016).**

1.1. Antibody-based immunotherapy against Tumor Associated Antigens

The conventional anti-cancer therapy includes surgery, radiotherapy, and chemotherapy; however, the main limits of the latter two conventional treatments are represented by the absence of selectivity for tumor cells and by non-specific side toxic effects. The immunotherapy targeting cancer cells, by the use of monoclonal antibodies specific for TAAs overexpressed on tumor cells, represent

an alternative strategy to overcome these limits. For this reason, the immunologists have worked with the aim of inducing specific immune responses against cancer, by developing drugs for targeted therapies **(Wurz et al. 2016; Kirkwood et al. 2012; Galluzzi et al. 2014).**

The targets of these therapies can be classified into Tumor Specific or cancer-testis Antigens (TSAs), expressed only on tumor cells, and Tumor Associated Antigens, overexpressed by tumors but present also at low levels on normal differentiated cells from which the tumors arise **(Wurz et al. 2016; Savage et al. 2014).**

The use of mAbs as magic bullets against these targets has rapidly increased over the last 40 years starting with the production of the first generation of therapeutic mAbs of mouse origin.

Unfortunately, the induction by human body of human anti-mouse antibody (HAMA) response represented an obstacle to the success of this approach and induced further research progresses to overcome these problems (**Thorpe et al. 2003).** Recombinant DNA technology allowed to replace the mouse costant domains, recognized by the human immune system, and responsible for HAMA response, with the human correspondent sequences, thus producing chimeric mAbs with reduced immunogenicity and improved pharmacokinetic and therapeutic efficacy **(LoBuglio et al. 1989).** Further improvements in recombinant DNA and cloning techniques led to humanized mAbs **(Carter et al. 1992),** obtained by inserting only the mouse hypervariable loops in the human V-region frameworks, thus further reducing the immunogenicity of the humanized antibodies.

More recently, new strategies, such as phage display technology, led to the generation of human antibody libraries, to be used for the *in vitro* selection of fully human antibodies specifically targeting tumor cells **(Frenzel et al. 2016).**

Some of the therapeutic mAbs approved by FDA for clinical use in cancer therapy are directed against either growth factors, such as vascular endothelial growth factor A, or growth factor receptors, such as human epidermal growth factor receptors EGFR and HER2/ErbB2. In addition to the specific and direct inhibitory effects on the signal transduction of these receptors expressed on tumor cells, therapeutic mAbs can also activate Antibody Dependent Cellular Cytotoxicity (ADCC) and Complement Dependent Cytotoxicity (CDC), or deliver towards tumor cells conjugated therapeutics, such as toxins or

radioisotopes. More recently, bispecific antibodies able to recognize two antigens have been created to retarget cytotoxic T lymphocytes to any cell of choice **(Wurz et al. 2016).**

1.2. ErbB2 and EGFR receptors as validated TAAs for breast cancer therapy

Worldwide, approximately 10 million people are diagnosed with cancer annually and more than 6 million die of this disease every year **(Stuart and Kleiheus 2006)**. In particular breast cancer affects one in eight women during their lives. It is the most common cancer in women worldwide, with nearly 1,8 million new cases (second most common cancer overall) diagnosed in 2013 **(Fitzmaurice et al. 2015).**

A good candidate as TAA and an attractive target for immunotherapy is ErbB2, a Tyrosine Kinase Receptor (RTK), overexpressed on many carcinoma cells, with a key role in the development of malignancies **(Slamon et al. 1989; Tagliabue et al. 1991; Lohrisch and Piccart 2001; Gravalos and Jimeno 2008).**

ErbB2 is a receptor belonging to the ErbB family of RTKs. Unlike the other members of the family, ErbB2 lacks natural ligands and acts as the preferential heterodimerization partner for the other members of the family. ErbB2 overexpression on tumor cells leads to the activation of intracellular tyrosine kinase domain and downstream signalling cascades that mediate cell growth, differentiation, and survival **(Yarden and Sliwkowski 2001; Klapper et al. 2000; Busse et al. 2000; Baselga et al. 2009)**, such as those of mitogen-activated protein kinase (MAPK) and phosphatidylinositol-3-kinase (PI3K) pathways (**Figure 3**), with a consequent dysregulated proliferation.

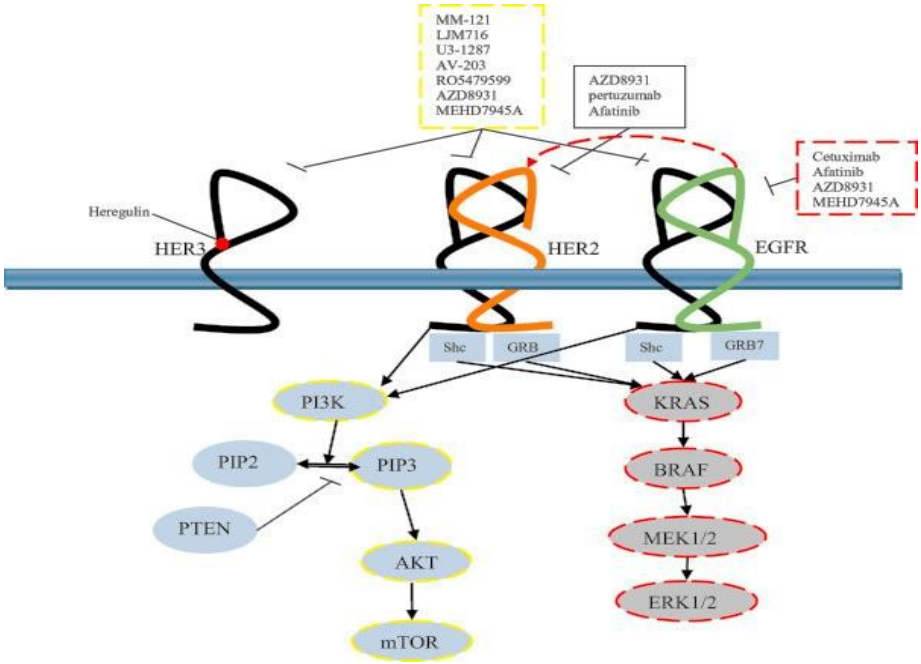

Figure 3. EGF receptor family. Schematic representation of the Tyrosine Kinase Receptors EGFR, ErbB2/HER2 and HER3, their downstream pathways and inhibitors **(Baselga J et al. 2009).**

Antitumor strategies have been well established for ErbB2-positive tumors and indicative examples include Trastuzumab, the first humanized antibody approved by the FDA in 1998 for breast cancer therapy, and Pertuzumab approved by FDA more recently for combinatorial treatments with Trastuzumab and Docetaxel **(Sabatier and Gonçalves 2014; Stebbing et al. 2000; Romond et al. 2005; Baselga and Swain 2010).** They have different mechanisms of action as they bind to different epitopes in the domain II and the domain IV of ErbB2, respectively. Despite the success of these antibodies for breast cancer their clinical efficacy is still limited by resistance and cardiotoxicity issues. Indeed, a high fraction of patients show resistance to their treatment and develop cardiac dysfunction, frequently leading to heart failure in particular in the presence of other

risk factors **(Slamon et al. 2001; Natha et al. 2006; Seidman et al. 2002; De Lorenzo et al. 2018).**

To overcome the limits of Trastuzumab, novel human antitumor immunoagents have been recently engineered in our laboratory by isolation of human single-chain variable fragments (scFvs) through phage display technology. In particular, a human anti-ErbB2 scFv, named Erbicin, was found to be able to selectively bind and inhibit ErbB2-positive tumor cells, and to recognize an epitope of ErbB2 different from that of Pertuzumab and Trastuzumab (**Figure 4**) **(De Lorenzo et al. 2002; Troise et al. 2011).**

The following fusion of Erbicin with the Fc region of a human IgG1 led to a new immunoagent construct, called Erb-hcAb (human compact antibody) for its compact size (100 kDa) if compared with the full size (155 kDa) of a natural IgG **(Figure 4).** This construct acquired the immune effector functions of the Fc domain while retaining the ability to diffuse more easily in the tumor masses due to its reduced molecular size with respect to a full size antibody. Erb-hcAb was found to selectively bind to breast tumor cells expressing ErbB2 and to inhibit their growth *in vitro* and *in vivo*, by inducing also Antibody Dependent Cellular Cytotoxicity (ADCC) and Complement-Dependent Cytotoxicity (CDC) **(De Lorenzo et al. 2004).** Interestingly, Erb-hcAb, differently from Trastuzumab and Pertuzumab, lacks cardiotoxic effects on human cardiomyocytes in *in vitro* and *in vivo* models **(Riccio et al. 2009; Fedele et al. 2012).**

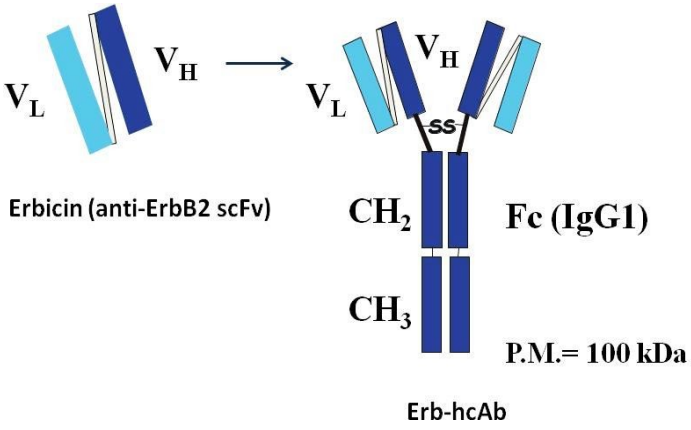

Figure 4. Erb-hcAb. Schematic representation of Erbicin and its derived compact antibody (Erb-hcAb).

Unfortunately, a high fraction of breast tumors does not express ErbB2. For instance, Triple-Negative Breast Cancer (TNBC), accounting for ~14% of all breast cancers, is characterized by the absence of Estrogen Receptor (ER), Progesterone Receptor (PR) and ErbB2, excluding the possibility of using efficacious targeted therapies developed against these proteins.

On the contrary, overexpression of EGFR has been reported in ~60% of TNBC and correlates with poor outcome. EGFR is the other member of the EGF tyrosine kinase receptor family, which also regulates the PI3K/AKT and Ras/MAPK signaling upon binding its ligand EGF and receptor dimerization. Increased EGFR expression may influence multiple aspects of tumor biology including cell proliferation, motility and invasiveness, and resistance to treatment (**Figure 3**) **(Stommel et al. 2007; Greenall et al. 2015; Haynes et al. 2014**).

Although more recently, also aptamers have raised increasing attention for cancer therapy due to their low molecular weight, lack of immunogenicity and ready availability. A RNA-aptamer, named CL4 (**Figure 5**), able to recognize and inhibit EGFR has been recently generated in the laboratory of our collaborators, by an *in vitro* selection procedure: SELEX (Systematic Evolution of Ligands by Exponential Enrichment) **(Tuerk and Gold 1990; Camorani et al. 2018; Camorani and Cerchia 2015).** The CL4 oligonucleotide aptamer was found able to bind and inhibit not only the human EGFRwt, but also the EGFRvIII mutant, expressed on the surface of Glioblastoma Multiforme (GBM) cancer cells, lacking most of the extracellular domain (**Esposito et al. 2011; Camorani et al. 2015)**. Indeed, it interacts with domain IV of the receptor, which is still present in the EGFRvIII variant, and inhibits the autophosphorylation of the receptor and its downstream ERK1/2 and STAT3 pathways, thus affecting migration and invasion of cancer cells **(Camorani et al. 2015)**. CL4 was also found able to inhibit the vasculogenic mimicry (VM) and tumor growth in TNBCs resistant to both Erlotinib and Cetuximab (EGFR-TK inhibitors), by preventing the EGFR-integrin αvβ3 interaction **(Camorani et al. 2017)**. Thus, its use could allow for overcoming the tumor resistance to EGFR Tyrosine Kinase Inhibitors (TKIs).

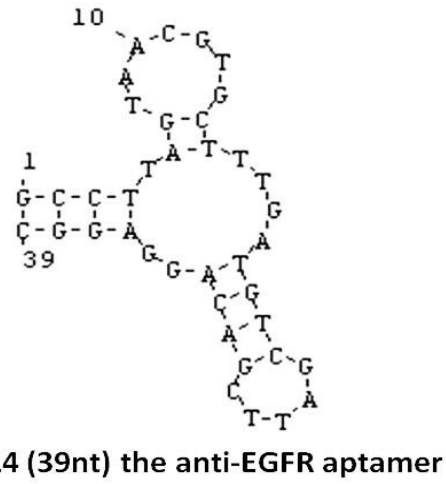

Figure 5. CL4 aptamer. Structure of the anti-EGFR CL4 aptamer **(Esposito et al. 2011).**

1.3. Immunotherapy targeting immune regulatory checkpoints

The other antibody-based approach in oncology exploits the activation of immune system, such as the stimulation of T cells mediated by immunomodulatory antibodies **(Peggs et al. 2009).**

Activation of immune cells involved in anti-tumor responses is regulated by multiple stimulatory and inhibitory pathways on effector T cells that can be targeted by monoclonal agonistic or antagonistic antibodies. The primary targets for such interventions were envisaged initially to be the effector T cells, but it is becoming clear that, also Natural Killer (NK) cells and regulatory T (Treg) cell populations might be important targets.

Understanding the complexity of immune regulation and tumor microenvironment has been critical to optimize the efficacy of the therapeutic approaches, and to develop new strategies for immune-based cancer therapy. The T cells have high specificity for their own antigen since they bear T cell receptors (TCRs) that specifically recognize cell-surface major histocompatibility complex

molecules associated with peptides derived from either endogenous or foreigner proteins.

Moreover, T cells are characterized by memory, because primary T cell responses are generally followed by the production of long-lived memory T cells with accelerated kinetics of response to a second presentation of the antigen **(Davis and Bjorkman 1988).** In order to induce the activation of effector T cells, the single engagement of the MHC by the recognition of associated antigenic peptides, such as those derived from TAAs, by the TCR is not sufficient for the full activation of T cells and may render them anergic. A series of various stimuli generated by co-regulatory signals are also required to fully activate T cells and to regulate their immune responses. These are exerted by a series of stimulatory or inhibitory receptor-ligand pairs and can determine the fate of the T cell response, such as their activation with the subsequent differentiation into effector T cells, their deletion or anergy **(Chen and Flies 2013)**.

Translation of this concept into the clinic has led the researchers to focuse their efforts on the identification of antibodies agonistic for co-stimulatory receptors or antagonistic for inhibitory signals, in order to use Immune Checkpoints (ICs) to amplify the antigen-specific T cell responses against cancer **(Pardoll 2012).**

To date, human or humanized mAbs targeting the immunosuppressive receptors CTLA-4 (Ipilimumab), PD-1 (Nivolumab and Pembrolizumab), and PD-L1 (Atezolizumab, Durvalumab and Avelumab) have been approved for the treatment of several tumors, including melanoma, non-small cell lung cancer, renal cell carcinoma, head and neck squamous cell carcinoma, Hodgkin lymphoma, urothelial carcinoma, liver carcinoma, microsatellite instable (MI) colorectal cancer and Merkel-cell carcinoma **(Brahmer et al. 2012; Patel et al 2017; Shultz 2017; Callahan et al. 2016).**

Despite their success, the currently approved antibodies against immune checkpoints (hence collectively named checkpoint inhibitors; CIs) are effective in only about 20-30% of the patients **(Lee et al. 2013; Buqué et al. 2015; Pardoll 2012).** As shown in **Figure 6,** new targets are emerging as co-inhibitory receptors, such as lymphocyte activation gene 3 (LAG-3), an immunosuppressive receptor expressed on activated T lymphocytes and T-regulatory

lymphocytes, T cell immunoglobulin and mucin-3 (TIM3), T cell immunoglobulin and ITIM domain (TIGIT), which are expressed on exhausted $CD8^+$ T cells in tumors **(Anderson et al. 2016; Goldberg and Drake 2011; Huang et al. 2004).** B- and T-lymphocyte attenuator (BTLA) is another co-inhibitory receptor whose expression is induced during activation of T cells, leading to inhibition of human $CD8^+$ cancer specific T cells **(Watanabe et al. 2003).** Similarly, some agonistic antibodies recognizing co-stimulatory receptors have reached the clinical stage such as those specific for OX40 (CD134), a secondary co-stimulatory immune checkpoint molecule that prevents premature death of activated lymphocytes, and 4-1BB (CD137) expressed on activated $CD4^+$ and $CD8^+$ T lymphocytes whose crosslinking enhances T cell proliferation, IL-2 secretion, survival and cytolytic activity. Other co-stimulatory proteins that are considered good targets for antibody-mediated immunotherapy are inducible T cell costimulator (ICOS), which is an immune checkpoint protein belonging to the CD28-superfamily that is expressed on activated T cells, and CD27, a member of the tumor necrosis factor receptor superfamily, which is required for generation and long-term maintenance of T cell immunity **(Chen and Flies 2013; Sanmamed et al. 2015; Wen et al. 2002; Sasso et al. 2018).**

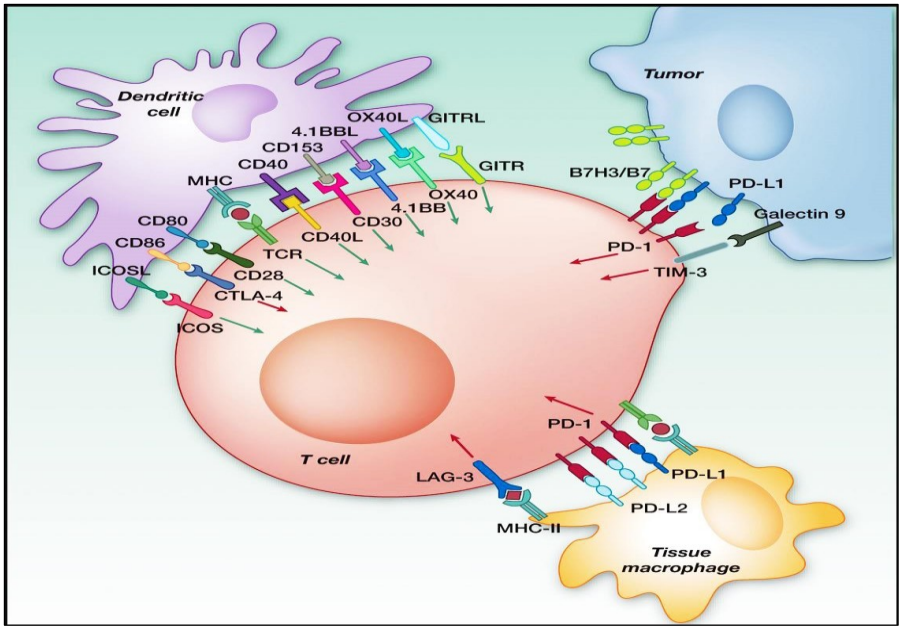

Figure 6. Potential immunomodulatory targets for monoclonal antibody-based therapy. The interaction between inhibitory receptors, such as CTLA-4, PD-1, BTLA, LAG-3, TIGIT, TIM-3 with their ligands leads to an inhibition of the T cell activation (red arrows). Co-stimulatory receptors such as CD28, ICOS, 4-1BB, OX40, CD27, on the contrary, enhance the effector function of T cells (green arrows).

Antibodies against different immune checkpoint receptors can also be combined to achieve additive or synergistic activity, potentially translating into a better efficacy. Proof of concept for this approach was provided by the finding of increased efficacy of the Ipilimumab and Nivolumab combination versus monotherapy in the treatment of metastatic melanoma **(Mahoney et al. 2015; Larkin et al. 2015).** A numerous clinical trials with approved or novel antibodies against immune checkpoints used in monotherapy or in combination with other biologics or small molecules are being carried out worldwide.

A new goal is represented by the generation of a complete repertoire of fully human antibodies specific for all these T cell

checkpoint modulators, so that they can be tested in all the possible combinatorial treatments **(Sasso et al. 2018).**

1.4. Generation of a human repertoire of mAbs for cancer therapy by Phage Display Technology

To obtain a repertoire of fully human immunomodulatory mAbs against several targets to be used in monotherapy or in combinatorial treatments with other anti-tumor drugs for cancer therapy, innovative strategies based on the well-known phage display technology have been considered in our laboratory.

Phage display is a precious technology that enabled to overcome the disadvantages of humanized mAbs, such as immunogenicity and low efficiency to penetrate tumor masses due to their large size (155 kDa), by producing fully human single chain variable fragments of antibodies and easily selecting them by affinity procedures.

The scFv is the smallest portion of the immunoglobulin, which retains the antigen-binding ability. Indeed, an antibody in the scFv format consists of variable regions of heavy (VH) and light (VL) chains, joined together by a flexible peptide linker, with a molecular weight of 27 kDa. Thanks to their low molecular weight and their retained property to bind to the antigen, the scFvs can be exploited in phage display technology to be expressed on the phage as fusion proteins with a protein of the phage coat, and to be selected for their binding to the targets **(Ahmad et al. 2012).**

Indeed, phage display is a strategy based on the expression of foreigner (poly)peptides on the surface of filamentous bacteriophages. This strategy was introduced in 1985, by George P. Smith, who demonstrated that the fragment of a protein could be expressed in a native conformation on the phage in order to be immunologically recognized by antibodies, with no significant effects on life cycle and infectivity of the phages **(Bazan et al. 2012).**

The gene encoding each scFv is packed inside the virion as a single-stranded DNA and the corresponding encoded protein is expressed as a fusion product with the pIII protein of the phage coat (**Figure 7**).

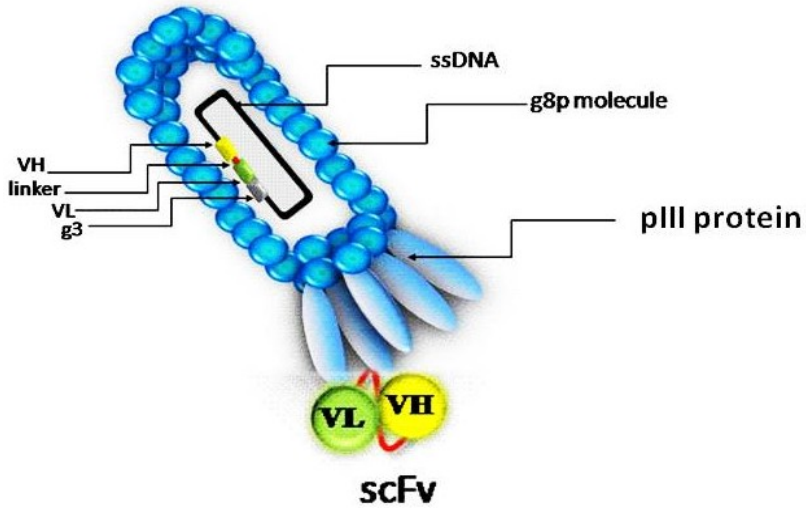

Figure 7. Schematic representation of scFv expressed as a fusion product with the pIII protein of the phage coat.

The phage display technology is based on the generation of libraries containing up to 10^{10} different variants, that can be used in a screening process to select antibodies against almost unlimited array of biological (including human self-antigens) and non-biological targets (such as toxic molecules). In order to identify the scFvs which specifically bind to the target, this technology allows for panning either on targets immobilized on solid support or expressed on the cell surface, by removing from the whole repertoire the non-binder clones by using affinity selection techniques.

In our laboratory a large number of anti-tumor or other anti-receptors scFvs have been successfully isolated by panning human scFv libraries either on purified proteins or on live cells expressing the targets on their surface **(De Lorenzo et al. 2002; Palmieri et al. 2015; Paciello et al. 2016).**

In the present project we tailored phage display to the generation of a complete repertoire of fully human antibodies

recognizing several different immune checkpoints. As shown in **Figure 8**, we applied for the first time a novel untested strategy for rapid, parallel screening of phage displayed antibody libraries by directly panning for the first time on activated human lymphocytes. This novel approach allows for the selection of antibodies recognizing the receptors in their native conformation, as that presented on the cell membrane, and to obtain a productive selection of several phage clones against multiple targets in one single panning.

As a proof of concept of the quality/potency of the binders identified by this approach, we generated fully IgGs from three of these collections i.e. PD-1, PD-L1 and LAG-3 (**Sasso et al. 2018)**. These three targets were chosen, as antibodies useful for biological assays and specific for them have been already developed by demonstrating therapeutic benefits, as described in the following paragraph.

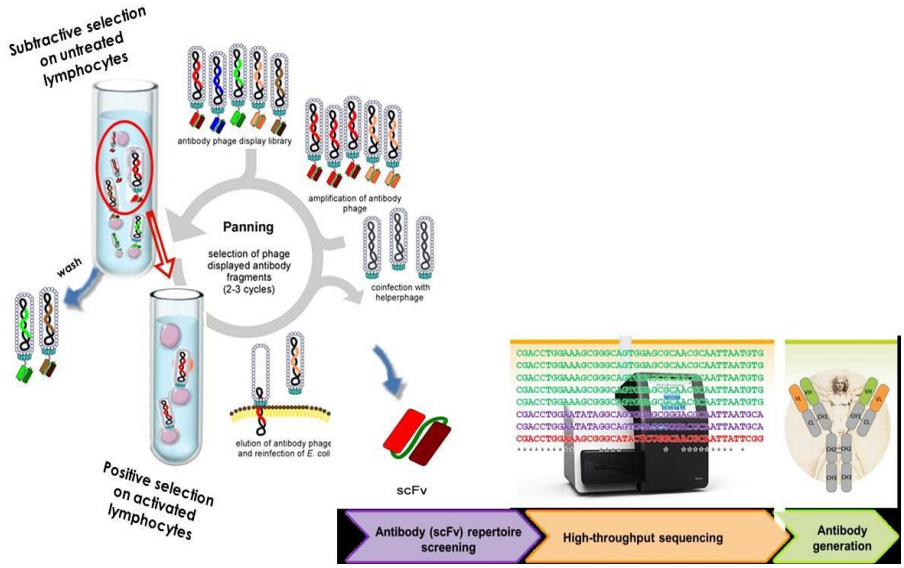

Figure 8. Strategy of scFvs selection by phage display against immune checkpoints. The phages were incubated with activated lymphocytes after a subtractive step on untreated lymphocytes in order to select specific phages for receptors expressed upon activation. The screening of enriched clones was performed by Next Generation Sequencing, and the identified scFvs were then converted into IgG4.

1.5. Programmed cell death receptor-1 (PD-1); Programmed Death Ligand-1 (PD-L1); Lymphocyte Activation Gene-3 (LAG-3) and their relative antibodies in use or clinical development

PD-1 is an immune checkpoint firstly identified in lymphoid cell lines undergoing programmed cell death. PD-1 is expressed on activated T-cells, B-cells, dendritic cells (DCs) and monocytes (**Figure 9**). The role of PD-1 on T-cells is to limit the activity of T-cells in peripheral tissues during inflammatory responses and to inhibit autoimmune responses. Its expression is induced when T cells become activated; therefore, when engaged by one of its ligands, such as PD-L1, PD-1 inhibits kinases that are involved in T cell activation **(Pardoll 2012).** This inhibition mechanism mediated by PD-1 can be exploited by the tumor cells expressing its ligand to neutralize the antitumor response of T cells **(Haile et al. 2013).**

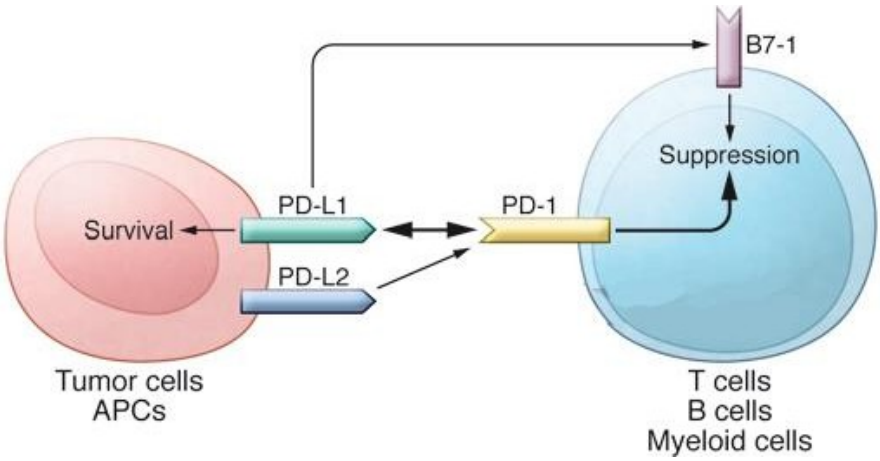

Figure 9. Schematic representation of PD-1/PD-L1 interaction and downstream effects. The interaction of PD-L1 or PD-L2 with PD-1 may induce T cell suppression.

Since, the interaction of PD-1, expressed on the surface of activated T cells, and PD-L1 on the surface of tumor cells results in immunosuppression, the interference mediated by an antibody specific for PD-1 could be a suitable strategy to reduce the

suppression of effector T cells. Two monoclonal antibodies targeting PD-1 have been already approved by the FDA: Pembrolizumab (Lambrolizumab) a humanized antibody firstly approved in 2014 to treat patients with unresectable or metastatic melanoma after treatment with Ipilimumab, and then approved in 2017 to treat also locally advanced or metastatic urothelial carcinoma **(Robert et al. 2014; Barnhart 2015; Shultz 2017),** and Nivolumab, a fully human mAb currently in clinical use for the therapy of Hodgkin lymphoma, unresectable or metastatic melanoma, metastatic renal cell carcinoma and non-small cell lung cancer (NSCLC) **(Raedler 2015; Kazandjian et al. 2016; Janice 2017).**

PD-L1 also acts as an inhibitor of human T cell responses, as the interaction of PD-L1 with PD-1 on activated T cells results in immunosuppression and tumor immune escape **(Assal et al. 2015).** PD-L1 is expressed on the surface of tumor cells (**Figure 9**) and its level was found increased in patients with cancer, likely because its expression is inducible by interferon γ (IFN-γ).

A number of antibodies targeting PD-L1 are in clinical development for metastatic melanoma, Non-Small Cell Lung Cancer (NSCLC), Renal Cell Cancer (RCC) and bladder cancer. For instance, Atezolizumab is a humanized anti-PD-L1 IgG1, approved by the FDA for non-small cell lung cancer in October 2016 and currently undergoing evaluation in clinical trials for patients with other types of cancer, including breast cancer, renal cell carcinoma, bladder cancer, and small-cell lung cancer **(Janice 2017).**

LAG-3, also known as CD223, is another negative regulator of T cell activation and homeostasis that was found to be specifically associated with the CD3–TCR complex following TCR engagement, and is therefore considered as a negative co-receptor (**Figure 10)**.

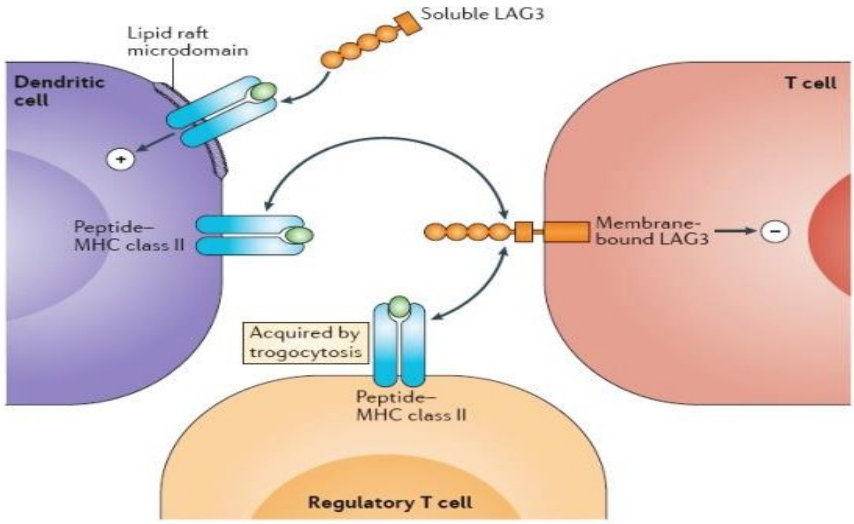

Figure 10. Schematic representation of LAG-3 and its interactions. LAG-3 is a transmembrane protein with structural homology to CD4, and four extracellular IgG domains. In addition to the membrane-bound form of LAG-3, it can be cleaved at the connecting peptide (CP) by metalloproteases to generate a soluble protein that functions as an immune adjuvant detectable in the serum.

LAG-3 is expressed on activated T cells, NK cells and B cells, and binds with high affinity to major histocompatibility complex (MHC) class II molecules (**Goldberg et al. 2011**). It has also been found on T_{Reg} cells, where it plays a role in amplifying the immunosuppressive activity of T_{Reg} cells, and in decreasing the pool of memory $CD4^+$ and $CD8^+$ T cells **(Huang et al. 2004).**

Furthermore, a monoclonal antibody targeting LAG-3, known as BMS-986016, is in phase 1/2a of clinical trials in monotherapy for advanced solid tumors (**ClinicalTrials.gov Identifier: NCT02966548. 2018**), and in combination with Nivolumab BMS-936558, in relapsed or refractory B-cell malignancies **(clinicaltrials.gov identifier: NCT02061761. 2018).**

1.6

AIMS

My PhD project was aimed at developing novel therapeutic approaches for cancer therapy by generating novel human antibodies.

An innovative trispecific multiparatope Tribody, targeting 3 nonoverlapping ErbB2 epitopes, was obtained in our laboratory in collaboration with a laboratory based in Lisbon. The first aim was the characterization of this novel Tribody by testing its ability to bind to tumor ErbB2-positive cells and to inhibit their growth.

A second aim was represented by the generation of a novel repertoire of fully human antibodies recognizing several different immune checkpoints in their native conformation. In this regard, the phases of the research activity were the following:

- set up of an innovative strategy based on phage display by performing a selection on hPBMCs;
- identification of the most enriched scFvs clones by NGS and bioinformatics;
- conversion of the selected scFvs into fully human IgG4;
- purification and characterization of the converted antibodies by: testing the binding affinity of each antibody by ELISA assays on lymphocytes and on purified proteins; analysing their ability to activate T cells, and evaluating their antitumor effects *in vivo*.

MATERIALS AND METHODS

Antibodies and human recombinant proteins

The following antibodies were used: horseradish peroxidase (HRP)-conjugated anti-His mouse monoclonal antibody (Qiagen); HRP-conjugated anti-M13 mouse monoclonal antibody (GE Healthcare); anti-human LAG-3 mouse monoclonal antibody (R&D Systems); anti-human PD-1 human monoclonal antibody Nivolumab (Opdivo®); anti-human PD-L1 human monoclonal antibody (G&P Biosciences); HRP-conjugated anti-human IgG (Promega); HRP-conjugated anti-human IgG (Fab')2 goat monoclonal antibody (Abcam); HRP-conjugated anti-rabbit immunoglobulin from goat antiserum (Thermo Fisher Scientific). Trastuzumab (Roche), Pertuzumab (Roche) Erb-hcAb (Biotecnol) **(De Lorenzo et al. 2004)**. Anti-ErbB2 rabbit monoclonal antibody and anti-pErbB2 rabbit polyclonal antibody were from Cell signaling Technology.

The following antibodies used for FACS analyses: PE/anti-human CD2 mouse monoclonal antibody (BioLegend), APC/anti-human CD3 mouse antibody, PE/anti-human CD4 mouse monoclonal antibody, PerCP/anti-human CD8 mouse monoclonal antibody were all from BD Biosciences.

APC/antihuman IgG Fc mouse antibody, APC/Cy7 anti-human CD366 (TIM3) mouse antibody, APC/anti-human CD272 (BTLA) mouse antibody, APC/anti-human CD137 (4-1BB) mouse antibody, APC/anti-human CD134 (OX40) mouse antibody, Brilliant Violet 510™/anti-mouse/rat/human CD27 hamster antibody, APC/antihuman/mouse/rat CD278 (ICOS) hamster antibody were all from BioLegend. FITC/anti-human TIGIT mouse antibody (Thermo Fisher Scientific).

The following recombinant chimeric proteins were used: human LAG-3/Fc; human PD-1/Fc; human PD-L1/Fc; TIM3/Fc; BTLA/Fc; TIGIT/Fc; OX40/Fc; 4-1BB/Fc; CD27/Fc and ICOS/Fc; human IgG1-Fc (all from R&D Systems) **(Sasso et al. 2018).**

Aptamers

2'F-Py RNA aptamers (CL4 and CL4Sc), used for treatments in cell viability assays, were synthesized by TriLink Biotechonologies. CL4Sc represents the scrambled form of CL4 and was used as a negative control. Before each treatment, the aptamers were subjected to a short denaturation-renaturation step (85°C for 5 min, on ice for 2 min, 37°C for 10 min).

Bacterial Culture Media

The bacterial growth was carried out in 2xTY and LB (Luria-Bertani) culture media.

Bacterial Strains

TG1 bacterial strain was used for the production of the scFvs expressed as fusion proteins with pIII protein of the phage; *E.Coli SF110* bacterial strain was used for expression of the scFvs as soluble proteins; *E. coli* DH5α (Invitrogen, Life Technologies, Paisley, UK) and BL21 DE3 strains (Novagen-Merck Millipore, Darmstadt, Germany) were used for cDNA amplification.

Antibiotics

The antibiotics used for bacterial growth and selection were Ampicillin (100 μg/ml) and Kanamicin (25 μg/ml).

Cell cultures

MDA-MB-231 and JIMT-1 cells were cultured in Dulbecco's Modified Eagle's Medium (GibcoTM DMEM, Thermo Fisher Scientific). MCF-7 cells were cultured in Modified Eagle's Medium (GibcoTM MEM, Thermo Fisher Scientific). SKBR3 cells (from ATCC, Rockville, MD) were cultured in RPMI 1640 (Gibco BRL,

Life Technologies, Paisley, UK). Media were supplemented with 10% (vol/vol) heat-inactivated fetal bovine serum (FBS, Sigma-Aldrich), 50 UI mL-1 penicillin, 50 µg mL-1 streptomycin (50 µg mL-1 streptomycin), 2 nM L-glutamine all from GibcoTM, Thermo Fisher Scientific. MCF7 cells trasfected with the cDNA encoding the variant of ErbB2 lacking exon16 (Δ16Her2) were grown in minimum essential medium (MEM) medium (Gibco BRL) supplemented with 10% heat-inactivated fetal bovine serum, penicillin (100 UI/mL), streptomycin (100 mg/mL), 2mM glutamine, 1mM sodium pyruvate, MEM aminoacids, and MEM nonessential aminoacids.

Production and Purification of Tribodies

Tribodies were produced by Biotecnol using its proprietary Trisoma platform, which includes proprietary expression and purification technology. This process recovers the Tribody L/Fd chain monomer while limiting impurities such as product variants and endotoxins. Tribodies were sterile filtered, aliquoted, and stored at 70°C. The purified tribodies were analyzed and confirmed to be >95% L/Fd chain Tribody monomer. Low levels of endotoxins were confirmed by a LAL-based method. Binding of the tribodies to their target was confirmed in an enzymelinked immunosorbent assays (ELISA) with a recombinant ErbB2 extracellular domain **(Riccio et al. 2017)**.

Western Blotting analyses for the detection of ErbB2 levels on tumor cells

The cells were plated ($6 \cdot 10^5$ cells/well) in 6-well plates and incubated at 37°C for 16 hours. Multiparatope and monoparatope tribodies (concentration of 10 nM) or each antibody (concentration of 10 nM) were added to the cells and incubated for 30 hours at 37°C. The treated cells were scraped and centrifuged at 1200 rpm for 7 minutes; the cell pellets were lysed in a buffer containing 10mM Tris-HCl (pH 7.4), 0.5% Nonidet-P-40, and 150 mM NaCl in the presence of protease inhibitors (Roche). After incubation on ice for 20 minutes,

the extracts were clarified by centrifugation at 12000 rpm for 15 minutes at 4°C. Protein concentration was determined by the Bradford colorimetric assay (Sigma-Aldrich) and Western Blotting analyses were performed by incubating the membranes with a commercial anti-ErbB2 antibody, followed by the HRP-conjugated secondary antibody, indicated above **(Riccio et al. 2017)**.

Cell Viability Assays to test the effects of the multiparatope Tribody on tumor cells

To test the effects of the multiparatope Tribody, or the combination of the 3 parental antibodies (Erb-hcAb, Trastuzumab and Pertuzumab) on tumor cell growth, SKBR3 cells were plated in 96-well flat-bottom at a density of $1.5 \cdot 10^4$/well and were incubated at 37°C for 72 hours with immunoagents (5–100 nM) in the culture medium. Cell counts were determined in triplicate by using the trypan blue exclusion test. Cell survival was expressed as the percentage of viable cells in the presence of the tested proteins, with respect to untreated control cultures **(Riccio et al. 2017)**.

Isolation of human Peripheral Blood Mononuclear Cells

Human PBMCs were isolated from blood of healthy donors by using Greiner Leucosep® tube (Sigma-Aldrich) following the manufacturer's instructions, and frozen in a solution containing 90% FBS and 10% dimethyl sulfoxide (DMSO) until use. Cryopreserved cell vials were gently thawed out by using RPMI 1640 medium (GibcoTM, Thermo Fisher Scientific) supplemented with 1% L-glutamine, 1% CTL-Wash™ (Cellular Technology Limited), and 100 U/mL Benzonase (Merck Millipore). The collected hPBMCs were then washed by centrifugation, plated and incubated overnight at 37°C in R10 medium consisting of RPMI 1640 supplemented with 10% inactivated FBS, 1% L-glutamine, 50 U mL-1 penicillin, 50 μg mL-1 streptomycin and 1% HEPES (GibcoTM, Thermo Fisher Scientific). After an overnight resting, the hPBMCs were collected in phosphate-buffered saline (PBS), counted by using the Muse® Cell Analyzer

(Merck Millipore), resuspended at a density of $1 \cdot 10^6$ cells/mL **(Sasso et al. 2018)**.

FACS analysis of expression levels of immune checkpoints on hPBMCs

Human PBMCs were isolated as described above. After an overnight incubation they were activated with Dynabeads® Human T-Activator CD3/CD28 at a concentration of $1 \cdot 10^3$ beads/mL (GibcoTM, Thermo Fisher Scientific). After 24-96 hours of activation, the cells were seeded in a round-bottom 96-well plate ($1 \cdot 10^6$ cells/well) and then centrifuged at 1200 rpm for 5 minutes to remove the supernatant. Unlabelled anti-LAG-3, anti-PD-1 (Nivolumab) or anti-PD-L1 primary antibodies were added to each well at a concentration of 10 µg/mL and incubated for 90 minutes at room temperature by gently shaking. After extensive washes, the cells were stained with 100 µL of APC/anti-human IgG Fc antibody in FACS buffer (PBS, 1% FBS), and with 10 µg/mL of PE/anti-human CD2 antibody (BioLegend, San Diego) for 45 minutes at room temperature by gently shaking. The labeled antibodies APC/Cy7 anti-human CD366 (TIM3), APC/ anti-human CD272 (BTLA), APC/ anti-human CD137 (4-1BB), PE/ anti-human CD134 (OX40), Brilliant Violet 510™/ anti-mouse/rat/human CD27, APC/ anti-human/mouse/rat CD278 (ICOS), FITC/ antihuman TIGIT antibodies were added to each well at a concentration of 10 µg/mL and incubated for 90 minutes at room temperature by gently shaking. After two washes with FACS buffer, the cells were resuspended in PBS and analyzed on CytoFLEX Flow Cytometer (Beckman Coulter). Lymphocytes were identified by analyzing the forward (FSC) versus side (SSC) scatter and gated to exclude debris. Healthy and apoptotic cell populations were identified by using viability staining (LIVE/DEAD solution, Thermo Fisher Scientific). The live cells only were considered to measure the percentage of positive cells corresponding to the fraction of cell populations double positive for both the expression of CD2 (the T-Lymphocytes lineage marker) and for the specific target of interest (LAG-3, PD-L1, PD-1, TIM3, BTLA, TIGIT, OX40, 4-1BB, CD27 or ICOS). Unstained cells or

cells treated with the appropriate isotype control were used as background control. Values were reported as the mean of at least three determinations (standard deviations ≤10%) **(Sasso et al. 2018)**.

Selection of scFv-phage clones

Phagemid particles were recovered from the library by using the M13-K07 helper phage (Invitrogen, Thermo Fisher Scientific), as previously described **(De Lorenzo et al. 2002)**. For each round of selection, phages (10^{13} cfu) were blocked by incubating them with 5% (wt/vol) Skim Milk Powder (Fluka Analytical, Sigma-Aldrich) for 30 mins in PBS before their use. For the first round of selection, blocked phages (10^{13} cfu) were firstly submitted to one round of negative selection by incubation with untreated lymphocytes ($5 \cdot 10^6$) in 2.5% (wt/vol) Skim Milk Powder (Fluka Analytical, Sigma-Aldrich, USA) in PBS for 2 hours at 4°C by gently rotation.

The unbound phages were collected in the supernatant by centrifugation at 1200 rpm for 10 minutes and then used for the positive selection, performed by incubating them with activated lymphocytes ($1 \cdot 10^6$) overnight by gently rotation at 4°C in the presence of 2.5% skim milk powder. For the selection of phages binding to CD27, BTLA and TIGIT the negative panning was not carried out to avoid the loss of some specific phages in the subtractive selection. After extensive washes with PBS, the bound phages were eluted from activated lymphocytes with 76 mM citric acid (pH 2.5) in PBS for 5 minutes, and then neutralized with 1M Tris-HCl (pH 8.0). The recovered phages were amplified by infecting *E. coli* TG1 cells to prepare phages for the next rounds of selection on the purified chimeric protein. To this aim, NuncTM polypropylene tubes (Fisher Scientific, Thermo Fisher Scientific) were coated with the selected recombinant chimeric proteins at a concentration of 20 μg/mL in a 0.05 M NaHCO3 solution, for 72 hours at 4°C. Blocked phages were submitted to two following rounds of negative selection by incubating them in the tubes coated with rhIgG1-Fc protein for 2 hours at 4°C in rotation.

Unbound phages, recovered in the supernatant, were then incubated in the coated tubes, prepared as described above for the

positive selection, overnight at 4°C in rotation, and eluted as described above. Alternatively, since a trypsin site is present between the scFv and the pIII protein of the phage coat, trypsin was used for a more efficient and selective elution of the binders. Briefly, after extensive washes with PBS, the bound phages were incubated with 50 mM Tris-HCl (pH 8.0) buffer containing 1 mM $CaCl_2$ for 1 hour at 4°C in rotation, and then eluted from the chimeric proteins with trypsin (1μg/mL), incubated for further 15 minutes at 25°C by gently shaking. The reaction was then blocked by using protease inhibitors (Complete™ EDTA-free Protease Inhibitor Cocktail, Sigma-Aldrich). Phages were then collected and stored at 4°C until use **(Sasso et al. 2018)**.

DNA fragment preparation and high-throughput sequencing

For each sublibrary, obtained from each selection cycle, the phagemid double-strand DNAs containing the scFvs were purified from cultures of superinfected *E. coli* TG1 cells using Endo free Plasmid Maxi Kit (Qiagen). The full-length scFvs were excised with restriction enzymes BamHI and HindIII, all from New England Biolabs, and purified with Wizard® SV Gel and PCR Clean-Up System (Promega) from 1.2% agarose gel **(Sasso et al. 2015).** A second enzymatic excision was performed with NcoI and XhoI, all from New England Biolabs, to isolate the VHs from the previously purified material, and then extracted from a 1,4% agarose gel. Library preparations for sequencing and preliminary bioinformatic analysis of the data were performed at the Center for Translational Genomics and Bioinformatics, Hospital San Raffaele, Milano, Italy. The VHs extracted from sub-libraries were bar-coded by TruSeq ChIP sample prep kit (Illumina). A complementary scheme for bar-coding was implemented to obtain a deep and suitable sequencing of VH mixtures of several subcycles. Subcycles 2 and 3 for each target were mixed in a dedicated run. The first universal cycle 1 was sequenced separately to cover the larger complexity. The bar-coded samples were diluted to a final concentration of 10 pM and sequenced with 2˙300 nt SBS kit v3 on an Illumina MiSeq apparatus **(Sasso et al. 2018)**.

scFv recovery

The clones of interest were isolated from the sublibrary at cycle 3 of the corresponding target. For high-ranking clones (relative representativeness ≥1% within cycle 3), the QuickChange II XL Site-Directed Mutagenesis Kit (Agilent Technologies) was used to perform copies of clones with overlapping primers, designed within the corresponding HCDR3 regions, according to the procedure previously described **(Sasso et al. 2015).** Briefly, the extension reactions were assembled as follows: 50-250 ng of template; 2/5 µL QuickSolution reagent; 1 µL *Pfu* Ultra High-Fidelity DNA polymerase (2.5 U/µL); 5 µL 10x reaction buffer; 1 µL dNTPmix; 125 ng forward primer; 125 ng reverse primer; H2O to a final volume of 50 µL. The template DNA was removed by restriction with 1 µL of *Dpn*I enzyme, as suggested by the kit provider. An appropriate amount of reaction was used to transform XL10-GOLD ultracompetent cells (Agilent Technologies) and then plated on LB/agar containing 100 µg/mL ampicillin. Some colonies were picked and evaluated by double digestion and sequencing. For low ranking clones (relative representativeness <1% within cycle 3), the DNA samples were isolated from cycle 3 by overlapping PCR. Briefly, Phusion High-Fidelity DNA Polymerase (Thermo Fisher Scientific) was used to perform two PCR reactions to obtain separately VH and VL fragments, using primers designed within the corresponding HCDR3 regions and in constant region of plasmid upstream and downstream of VH and VL.

In a second step, the PCR fragments corresponding to each clone were mixed and extended to get the full scFvs. The reactions were assembled as follows: 150 ng of template for VH and VL fragments amplification and 10 ng of template (VH and VL fragments) for full scFv amplification; 0.5µL Phusion DNA Polymerase (0.02 U/µl); 10 µL 5X Phusion HF Buffer; 1 µL dNTP mix; 0.5 µM forward primer; 0.5 µM reverse primer; 1.5 µL DMSO; H2O to a final volume of 50 µL **(Sasso et al. 2018)**.

Antibody production and purification

The scFvs of interest were converted into whole IgG4 antibodies by cloning the corresponding VH and VL cDNAs in the pEU vectors 8.2VH and 4.2VL, expressing respectively, the constant antibody heavy and light chains **(Paciello et al. 2016)**. Briefly, the VHs and VLs were amplified by CloneAmp HiFi PCR Premix in standard conditions with specific primers and purified by Wizard® SV Gel and PCR Clean-Up System (Promega) from 1.3% agarose gel.

In-Fusion HD cloning kit (Clontech Laboratories) was used to clone the VHs in *Bam*HI and *Bss*HII (New England Biolabs), linearized pEU8.2VH vector, and the VLs in *Apa*LI and *Avr*II (New England Biolabs), linearized pEU4.2VL vector. Stellar Competent Cells (Clontech Laboratories) were transformed with the obtained vectors, and the colonies were screened by digestion and sequence analysis. The vectors containing the correct DNA, prepared with an endotoxin-free system (EndoFree Plasmid Maxi Kit, Qiagen), were co-transfected in HEK293-EBNA by using Lipofectamine Transfection Reagent (Life Technologies, Inc.) and grown up for about 10 days at 37°C in chemical defined CD CHO medium (Gibco, Life Technologies, Inc.) supplemented with 5 mL of L-glutamine 200 mM (Gibco, Life Technologies), 5 mL of Penicillin (100 UI/mL) and Streptomicyn (100 mg/mL), from Sigma-Aldirch, in 6-well plates or in 150 mm Corning® tissue-culture treated culture dishes.

The conditioned media were collected, and the antibodies were purified by using Protein A HP SpinTrap30 (GE Healthcare Life Sciences). The purity of the final products was evaluated by SDSPAGE NuPAGE™ 4-12% Bis-Tris Protein Gels, 1.0 mm, 10-well (Thermo Fisher Scientific) followed by the staining with Coomassie blue solution (Biorad) for 20 minutes and de-stained with 7% CH3COOH and 20% Et-OH. All the antibody preparations were filtered with sterile 0.22 μm durapore hydrophilic filters (Millipore) before their use **(Sasso et al. 2018)**.

Enzyme-Linked Immunosorbent Assays (ELISA)

To detect the surface ErbB2 levels on ErbB2-positive cells, the cells were harvested in nonenzymatic dissociation solution (Sigma-

Aldrich), washed and plated in 96-well round-bottom microtiter plates ($2 \cdot 10^5$ cells/well). Then, the cells were incubated in the absence or presence of increasing concentrations of each Tribody (3–100 nM) or other anti-ErbB2 antibodies (in ELISA buffer PBS/BSA 3%) at room temperature for 2 hours **(Riccio et al. 2017).**

To confirm the binding specificity of the purified immunomodulatory mAbs, ELISA assays were performed on chimeric proteins (coated at 5 μg/mL on microplates), tumor cells (PD-L1-positive breast cancer MDA-MB-231 or PD-L1-negative breast cancer MCF7 cells), and untreated or activated hPBMCs.

The ELISA assays on coated chimeric protein were performed by coating NuncTM flat bottom 96-well plates (Thermo Fisher Scientific) with 5 μg/mL rhPD-L1, rhPD-1 and rhLAG-3 recombinant proteins in a solution of 0,05 M NaHCO3 for 72 hours at 37°C. After blocking of the coated 96-well plates with 5% nonfat dry milk in PBS for 1 hour at 37°C, the purified mAbs were added at increasing concentrations (10-200 nM) to the plates in 2.5% nonfat dry milk in PBS and incubated for 2 hours at room temperature by gently shaking.

Cell ELISA assays were performed by plating the cells in round-bottom 96-well plates ($2 \cdot 10^5$ cells or $2 \cdot 10^5$ lymphocytes for each well) and incubating them with increasing concentrations (0.5-200 nM) of mAbs in 2.5% nonfat dry milk for 2 hours at room temperature with gentle agitation **(Sasso et al. 2018)**.

After the incubation with the primary antibodies extensive washes were carried out with PBS, then the plates were incubated with an appropriate HRP-conjugated antibody for 1 hour at room temperature, washed again and incubated with 3,3',5,5'-tetramethylbenzidine (Sigma-Aldrich) reagent for 10 min before quenching with an equal volume of 1 N HCl. Absorbance at 450 nm was measured by the Envision plate reader (Perkin Elmer, 2102). Binding values were reported as the mean of at least three determinations obtained in three independent experiments.

The Kd values were calculated by elaboration of ELISA binding curve analyses by Prism (Graphpad) tool according to the following model: Y=Bmax*X/(Kd+X) + NS*X + Background. Bmax is the maximum specific binding in the same units as Y; Kd is the equilibrium binding constant, in the same units as X, and it is the ligand concentration needed to achieve a half-maximum binding at

equilibrium; NS is the slope of non-specific binding in Y units divided by X units; background is the amount of nonspecific binding with no added ligand.

Competitive ELISA assays

In order to investigate the ability of the selected PD-L1_1 and PD-L1_2 antibodies to compete in the PD-L1/PD-1 or PD-L1/B7.1 binding, competitive ELISA assays were performed by testing the binding of each biotinylated chimeric protein (PD-1/Fc or B7.1/Fc) to PD-L1 in the absence or in the presence of the unlabelled competitive antibodies. To this aim, a NuncTM flat-bottom 96-well plate was coated with 200ng/ml of PD-L1 recombinant protein in 0.005M $NaHCO_3$ solution for 72 hours at 4°C. Then, the PD-L1 coated plate was pre-incubated with the competitor PD-L1_1 and PDL1_2 antibodies (at 10:1 M/M excess ratio), and then further treated with the biotinylated PD-1 or B7.1 chimeric proteins, which were added to the plate at the same concentrations of the competitive antibodies (2μg/ml corresponding to $2.4 \cdot 10^{12}$ molecules/well). For the detection of bound biotinylated proteins, HRP-conjugated Streptavidin (Biorad) was added to the plate, whereas an anti-human antibody was used in parallel assays for the detection of bound anti-PD-L1 antibodies.

To determine whether the novel anti-PD-1 mAbs recognize different epitopes from that recognized by Nivolumab, competitive ELISA assays were performed on plates coated with PD-1/Fc chimeric protein (5 μg/mL). After blocking with 5% Nonfat Dry Milk in PBS, the coated 96-well plate was pre-incubated for 2 hours with saturating concentrations of each unlabelled mAb (400 nM) in 2.5% Nonfat Dry Milk in PBS in agitation at room temperature. After extensive washes with PBS, increasing concentrations of biotinylated Nivolumab mAb were added. For the detection of the binding, the plate was incubated with HRP-conjugated Streptavidin for 30 minutes in agitation at room temperature, washed again and analyzed as described above **(Sasso et al. 2018)**.

Lymphocyte proliferation assays by FACS analysis

For the staining, pre-warmed 0.1% bovine serum albumin/PBS solution containing CFDA-SE (Vybrant® Cell Tracer Kit, InvitrogenTM, Thermo Fisher Scientific) at a concentration of 10 μM was used to resuspend hPBMCs at a density of $1 \cdot 10^6$ cells/mL, that were incubated at 37°C for 10 minutes. Ice-cold R10 medium was then used to permeabilize the cells by incubating on ice for an additional 5 min. The cells were then washed three times with PBS. Between the second and the third wash, the cells were incubated at 37°C for 5 minutes to allow for the complete removal of excess of CFDA-SE. After the last wash and centrifugation at 1200 rpm for 10 minutes, the cells were resuspended at a density of $1 \cdot 10^6$ cells/mL in R10 and plated into a 48-well plate ($1 \cdot 10^6$ cells/well). The lymphocyte proliferation assays were performed by incubating the plated lymphocytes with 2.5 μg/mL phytohemagglutinin-L (PHA-L, Roche), in the absence or in the presence of the selected anti-LAG-3, anti-PD-1 or anti-PDL1 mAbs (10 μg/mL). The plates were then incubated at 37°C for 5 days. At the end of treatment, each sample was recovered, resuspended in 100 μL of PBS and transferred into a round-bottom 96-well plate. First, the cells were incubated with violet LIVE/DEAD solution (Thermo Fisher Scientific) for 30 minutes at 4°C. After several washes, the samples were further incubated with the anti-human CD3 (APC), anti-CD4 (PE) and anti-CD8 (PerCP) antibodies (10 μL/sample) for 1 hour at 4°C. Finally, the cells were extensively washed, resuspended in 200 μL of PBS and transferred into 5 mL polystyrene round-bottom tubes (BD Biosciences) for acquisition at CytoFLEX Flow Cytometer (Beckman Coulter) **(Sasso et al. 2018)**.

Effects of novel antibodies on the production of cytokines by stimulated hPBMCs

hPBMCs ($1 \cdot 10^6$ cells) were cultured and stimulated with 2.5 μg/mL PHA-L or 50 ng/ml Staphylococcal enterotoxin B (SEB, Sigma-Aldrich) for 18, 42 and 66 hours, in the absence or in the presence of the selected anti-LAG-3, anti-PD-L1 and anti-PD-1 mAbs (20 μg/mL) or an isotype control antibody, used as a negative control.

Nivolumab and Atezolizumab (InvivoGen, hpdl1-mab 9-1) were tested as a positive control in parallel assays, in the same conditions. The levels of IL-2 or IFNγ in cell culture supernatants were measured by ELISA assays (all from DuoSet ELISA, R&D Systems), according to the manufacturer's recommendations. Concentration values were reported as the mean of at least three determinations in five independent experiments performed by using lymphocytes from 5-8 healthy donors **(Sasso et al. 2018)**.

Lymphocyte proliferation ELISA assay based on the measurement of BrdU incorporation after co-culture with PD-L1 positive tumor cells

Since the MDA-MB-231 breast tumor cells express high levels of PD-L1 molecules on their surface, we tested the ability of the anti-PD-L1_1 and PD-Ll_2 antibodies to suppress the inhibitory action of the PD-1/PD-L1 interaction on lymphocyte proliferation when the two cell types are co-cultured. To this aim we performed a colorimetric immunoassay, by using the Cell Proliferation ELISA BrdU kit (Roche® Applied Science GmbH), according to the manufacturer's recommendations, for the quantification of the lymphocyte proliferation. Briefly, MDA-MB-231 ($1\cdot10^4$ cells/well) were previously treated for 30 min at 37°C with mitomycin C (50 μg/ml), which inhibits the DNA synthesis of tumor cells, thus allowing for the specific evaluation of lymphocyte proliferation. Then, the tumor cells were co-cultured with hPBMCs in the absence or in the presence of increasing concentrations of anti-PD-L1 antibodies (50, 100 and 200 nM) for 72 hours at 37°C. After an additional incubation of 24 hours with BrdU labelling solution, the cells were fixed and the DNA was denatured to improve the accessibility of the BrdU incorporated in newly synthesized DNA for detection with the HRP-conjugated anti-BrdU antibodies. The bound antibodies were detected by the addition of TMB and quantified spectrophotometrically by measuring the absorbance at 450 nm. The increase of the absorbance values correlate with DNA synthesis, and thus allow for quantification of proliferating cells **(Sasso et al. 2018)**.

In vivo studies

Six-week old female BalBC mice (Envigo) were used for *in vivo* studies. Mice were implanted subcutaneously on the right flank with $2 \cdot 10^5$ CT 26 tumor cells (day 0), and then treated intra-peritoneally with 200 μg of α-mPD-L1 (BioXcell, clone 10F.9G2), α-mPD-1 (BioXcell, clone RMP114), PD-1_1 or PD-L1_1 at day 3, 6 or 10. Tumor growth was measured by caliper every 3-4 days using the formula LxW2/2 (L as the largest and W the smallest diameter of the tumor). Animals were sacrificed as soon as signs of distress or a tumor volume above 2000 mm^3 occurred **(Sasso et al. 2018).**

Statistical analyses

Error bars were calculated on the basis of the results obtained by at least three independent experiments. Analyses on activated lymphocytes were performed by using samples of hPBMCs obtained by at least three different donors. For these studies, differences between groups were assessed by Student's *t*-test. Statistical significance was defined as $p<0.05$.

RESULTS

1. Immunotherapy based on novel human immunoagents specific for TAAs

1.1 In Vitro Effects of the Triparatopic Targeting Tribody on Tumor Cell Growth

Combinations of antibodies targeting different epitopes on the same Tyrosine Kinase receptor extracellular domain are often able to downregulate oncogenic activity more efficiently than single mAbs by increasing internalization and degradation of the receptor, as well as by preventing the activation of the tyrosine kinase activity **(Drebin et al. 1988; Friedman et al. 2005; Scheuer et al. 2009)**.

The hypothesis was formulated in our laboratory that trispecific molecules, including binding sites for three different epitopes of the same receptor, can bind almost the double amount of receptors and can do that in such a way that a more complex and dense matrix is formed **(Figure 11F) (Riccio et al. 2017)**.

To test whether the simultaneous targeting of 3 nonoverlapping ErbB2 epitopes in a trispecific molecule, showed more efficient antitumor properties than that of a monospecific trivalent molecule with 3 identical binding sites recognizing one epitope only, different tribodies were produced. Tribodies are novel biological constructs, made up of a Fab fused to two scFvs, as they consist of a light chain (L) containing an N-terminal variable (VL) domain and a C-terminal constant (CL) domain and a Fd chain including 2 N-terminal variable (VH) and C-terminal constant (CH1) domain. Both the L and Fd chains are extended at their C-termini with a flexible linker joining each of them with an additional scFv **(Figure 11)**.

Three different tribodies were designed and constructed in collaboration with a research group (based in Lisbon): a trispecific multiparatope Tribody (Tb), called Tb-TPE, which targets the 3 different epitopes recognized by Trastuzumab (T), Pertuzumab (P), and Erbicin (E), respectively. As controls, their 3 corresponding

trivalent monoparatope tribodies, Tb-TTT, Tb-PPP, and Tb-EEE were produced (**Figure 11D**) **(Riccio et al. 2017)**.

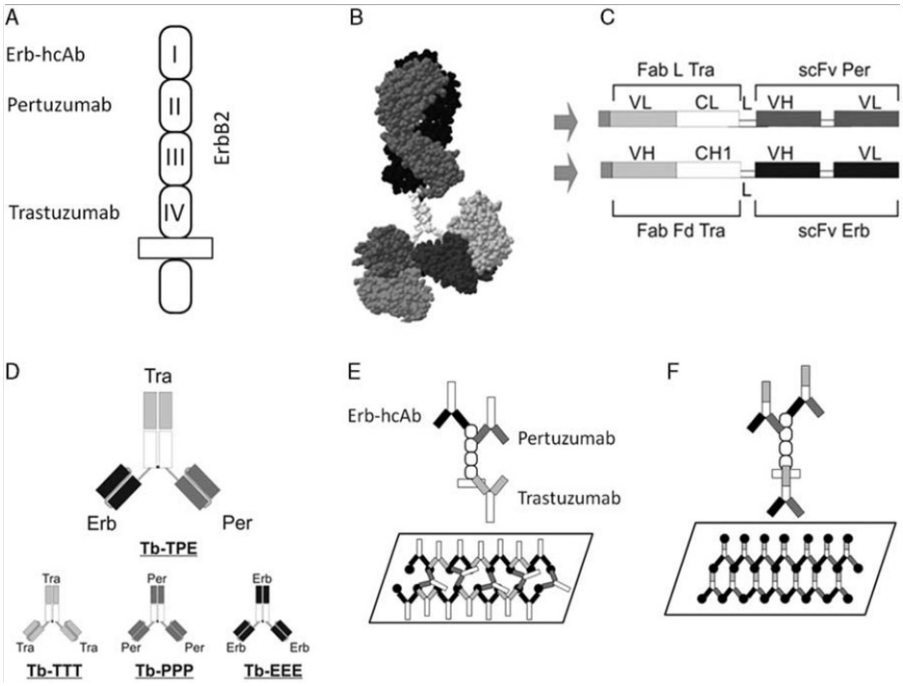

Figure 11. Triparatopic Tribody specific for ErbB2. A: Schematical representation of ErbB2: the epitopes recognized by the antibodies are in domain I (Erb-hcAb), domain II (Pertuzumab), and domain IV (Trastuzumab) of the ErbB2 extracellular domain. B: Tribodies are stable and flexible antibody derivatives with a long span of each consisting of a recombinant fusion of a Fab fragment with 2 different scFv fragments at their C-terminus.The model shown was based on a mouse anti-chicken egg lysozyme Fab (PDB 1FDL) and scFv (PDB 2ZNX) using PyMOL. C: Tribodies are constructed by genetic fusion of the genes for either the Fab Fd-chain or L-chain with the genes of 2 distinct scFv molecules. D: The triparatopic Tb-TPE (trivalent Tribody made up of 3 binding sites recognizing distinct nonoverlapping epitopes of ErbB2, derived from Erb-hcAb (in black), Pertuzumab (in gray), and Trastuzumab (in light gray) was compared with the trivalent monoparatopic equivalents Tb-TTT, Tb-PPP, and Tb-EEE. The schematic model of a possible aggregation induced by 3 pairs of bivalent monoparatopic mAbs (E) or by triparatopic molecules (F) **(Riccio et al. 2017)**.

Binding assays to evaluate and compare the ability of the monoparatopic versus triparatopic Tribodies to bind to ErbB2-positive tumor cells were also previously carried out by my colleagues in our laboratory. A positive correlation between the levels of expression of ErbB2 on a cell line and the binding of the tribodies to the cells was observed, thus confirming their binding specificity for the target. Moreover, the triparatopic tribody showed the highest affinity for all the cell lines tested (**data not shown**) **(Riccio et al. 2017)**.

Furthermore, the multiparatope and monoparatope tribodies were also previously tested by my colleagues to evaluate their effects on a panel of ErbB2-positive tumor cells. With this aim the cells were incubated for 72 hours in the absence or in the presence of increasing concentrations of each immunoagent and cell survival was evaluated by trypan blue cell counts. The multiparatope tribody Tb (TPE) strongly inhibited the growth of all the tumor cells tested, including those resistant to Trastuzumab, differently from Tb (TTT). As for the tumor cells sensitive to Trastuzumab, the triparatope tribody showed a stronger cytostatic activity at low concentrations, than that of monoparatope tribodies **(data not shown, Riccio et al. 2017)**.

1.2 Receptor Downregulation is Enhanced by Triparatopic Tribody

To test whether the effects of Tb (TPE) on tumor cell growth was due to its ability to downregulate the levels of ErbB2 more efficiently then the monoparatope tribodies, mammary SKBR3 tumor cells were treated with multiparatope or monoparatope tribodies for different time intervals (16, 30, 48, 60, and 72 hours). Cells were then lysed and the level of ErbB2 was evaluated by western blotting analysis with a commercial anti-ErbB2 antibody. The level of ErbB2 in SKBR3 cells treated with the multiparatope Tribody Tb-TPE was significantly downregulated after 30 hours, while the monoparatope tribodies did not downregulate ErbB2 so efficiently **(Figure 12)**. Similar results were obtained also for the longer time intervals used (**data not shown**) **(Riccio et al. 2017)**.

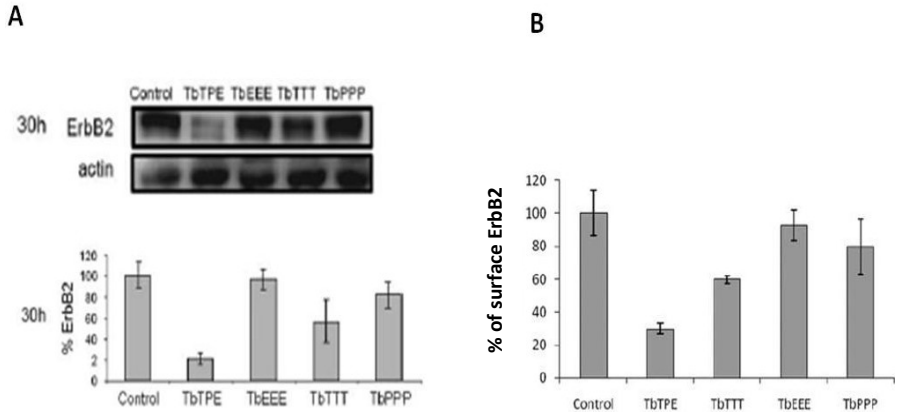

Figure 12. Effects of the tribodies on ErbB2 downregulation on tumor cells. A: Western blotting analyses with an anti-ErbB2 antibody of extracts from SKBR3 tumor cells untreated (control) or treated with the indicated tribodies for 30 hours at 37° C. The intensity of the bands was normalized with actin used as standard protein and reported as percentages of the ErbB2 levels detected in untreated cells (lower panel). B: Cell ELISA assay with an anti-ErbB2 antibody to detect the surface receptor on SKBR-3 tumor cells treated with the indicated tribodies for 30 hours at 37°C. The absorbance values, measured by a microplate reader, are reported as percentage of the surface ErbB2 levels with respect to those detected in untreated cells (control). The values were reported as the mean of at least three determinations obtained in three independent experiments. Error bars depicted means ± SD **(Riccio et al. 2017)**.

As control, SKBR-3 cells were also treated with the multiparatope Tribody in the absence or presence of an excess (10:1 M/M) of each Fab (Erb-Fab, Tra-Fab, Per-Fab) to confirm that all the 3 epitopes are needed to efficiently downregulate ErbB2 levels. Indeed, the downregulation of ErbB2 in the cells treated with the multiparatope Tribody is significantly inhibited only by the combination treatment with all 3 Fabs, but it is not affected by the cotreatment with 1 Fab only (**data not shown**) (**Riccio et al. 2017**).

We also compared the effects of the multiparatope Tribody on downregulation of ErbB2 in SKBR3 cells with those resulting from the effects of treatment with the combination of the 3 antibodies targeting different epitopes (Erb-hcAb, Trastuzumab, 2C4 or

Pertuzumab). As shown **in Figure 13A**, the multiparatope Tribody downregulates ErbB2 more efficiently than the combinatorial treatment of the 3 different antibodies. To test whether these effects on ErbB2 downregulation were correlated to those on cell viability, the same combinatorial experiments were repeated as described above, and the cell survival was measured by trypan blue cell counts. The multiparatope Tribody inhibits the tumor cell growth more efficiently than each combinatorial treatment, thus suggesting that its more potent effect on receptor degradation leads to a more potent antitumor effect (**Figure 13B).** These results strongly indicate that the multiparatope Tribody combines and enhances the therapeutic effects of the 3 different antibodies in 1 single antibody construct **(Riccio et al. 2017)**.

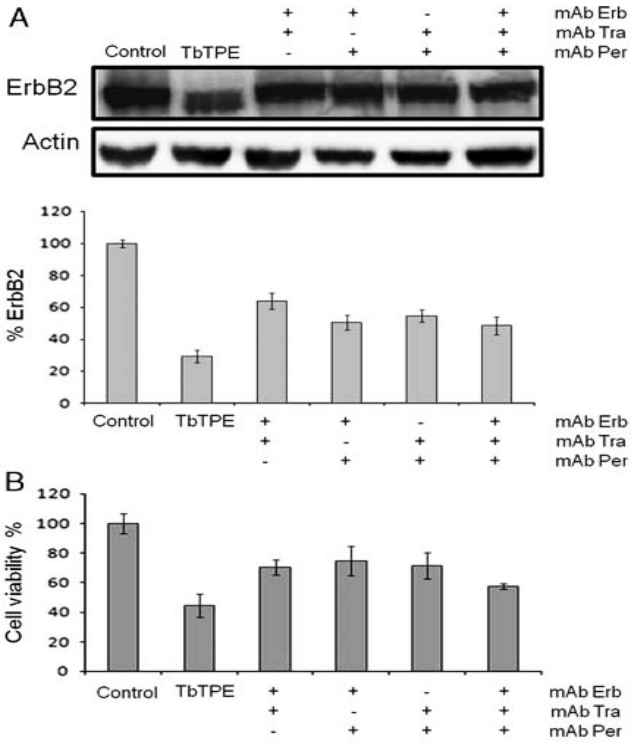

Figure 13. Comparison of the effects of the trispecific Tribody with respect to the combination of the 3 parental antibodies on ErbB2 downregulation and cell viability. A: Western blotting analysis with an anti-ErbB2 antibody of extracts from SKBR3 cells treated with the multiparatope Tribody or with the combination of the indicated antibodies. The intensity of the bands was normalized to actin and reported as percentages of the ErbB2 levels detected in untreated cells (lower panel). B: Viability of SKBR3 cells treated with the multiparatope Tribody or with the combination of the indicated antibodies is reported as a percentage of cell viability of untreated cells. The values were reported as the mean of at least three determinations obtained in three independent experiments. Error bars depicted means ± SD **(Riccio et al. 2017)**.

We further evaluated whether the levels of ErbB2 were downregulated in Trastuzumab-resistant MCF7-HER2Δ16, and JMTI-1 cell lines. MCF7-HER2Δ16 is a cell line expressing the variant of HER2Δ16, encoding a receptor lacking exon 16, the absence of which

determines constitutive active dimers with transforming activity **(Mitra et al. 2009)**. JIMT-1 cells express high levels of MUC4, which masks the epitope recognized by Trastuzumab **(Nagy et al. 2005)**.

These cells were incubated in the absence or in the presence of 10 nM triparatope (Tb-TPE) or monoparatope tribodies for 30 hours at 37°C. In a parallel assay, SKBR-3 cells were used as a positive control.

As shown **in Figure 14**, the level of ErbB2 in MCF7-HER2Δ16 cells treated with the triparatope Tribody Tb-TPE is dramatically reduced, whereas it is not affected by the treatment with monoparatope tribodies, with the only exception of the treatment with Tb-EEE. Similar results were also obtained with the triparatope Tribody Tb-TPE on JIMT-1 cells**,** which were found to be sensitive to treatment with Tb-EEE but unaffected by Tb-TTT, as expected by taking into account the resistance of these cell lines to Trastuzumab.

To confirm these results with another experimental approach that allows for the detection of the levels of the receptor expressed only on the cell surface, we repeated the experiment mentioned above by performing cell ELISA assays with an anti-ErbB2 mAb on both Trastuzumab-resistant MCF7-HER2Δ16, JMTI-1 or Trastuzumab-sensitive SKBR3 tumor cells, previously treated in the absence or in the presence of 10 nM triparatope (Tb-TPE) or monoparatope tribodies for 30 hours at 37°C. The results are comparable to those obtained by western blotting analyses **(Figure 14)**, and strongly indicate that Tb-TPE reduces the density of the cell surface receptor on all the cell lines tested more efficiently with respect to the monoparatope tribodies **(Riccio et al. 2017)**. Thus, we can conclude that a triparatope Tribody specific for ErbB2 has the potential to become a best-in-class therapeutic to address monotherapy drug resistance and tumor heterogeneity.

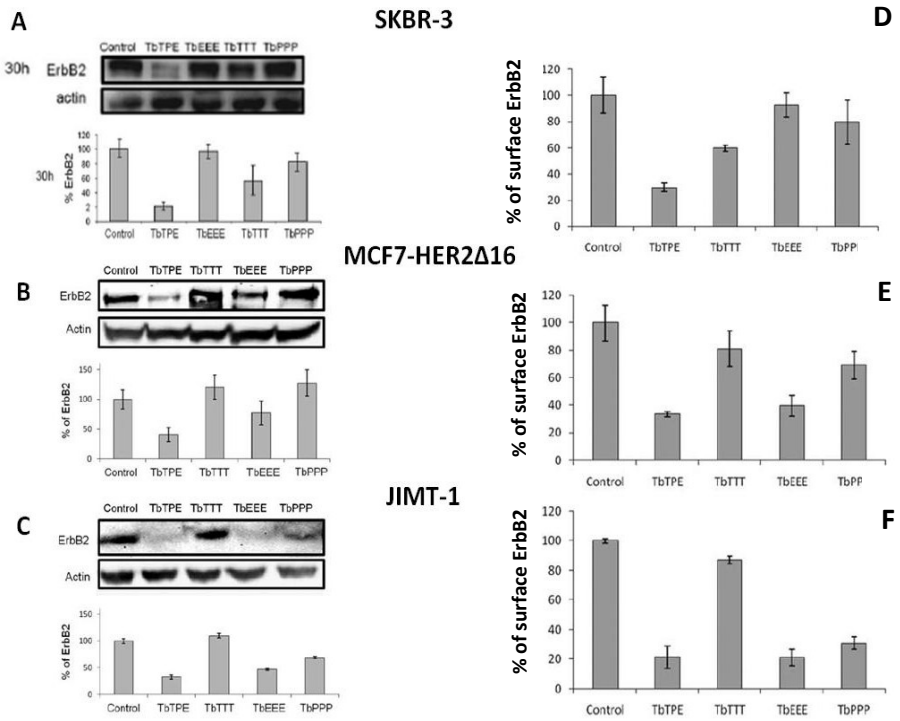

Figure 14. Effects of the tribodies on ErbB2 downregulation on tumor cell lines. On the left, Western Blotting analyses with an anti-ErbB2 antibody of extracts from SKBR-3 (A), MCF7-HER2Δ16 (B), JIMT-1 (C) tumor cells untreated (control) or treated with the indicated tribodies for 30 hours at 37° C. The intensity of the bands was normalized with actin used as standard protein and reported as percentages of the ErbB2 levels detected in untreated cells. On the right, cell ELISA assays with an anti-ErbB2 antibody on SKBR-3 (D), MCF7-HER2Δ16 (E), JIMT-1 (F) tumor cells treated with the indicated tribodies for 30 hours at 37°C. The absorbance values measured by a microplate reader are reported as percentage of the surface ErbB2 levels detected in untreated cells. The values were reported as the mean of at least three determinations obtained in three independent experiments. Error bars depicted means ± SD **(Riccio et al. 2017)**.

2. Immunotherapy based on immunomodulatory mAbs

2.1 Selection of scFvs on activated human PBMCs

Our goal was the generation of a repertoire of human antibody against immune checkpoints. Since many IC are expressed on the surface of T lymphocytes and their expression is increased when T cells are exposed to antigen-dependent or independent stimuli, we sought to use unfractionated human peripheral blood mononuclear cells (hPBMCs) to screen libraries of human scFvs. To optimize the selection process, we first evaluated the kinetics and level of expression of 10 different IC **(Table 2)** after *in vitro* activation with anti-CD3/CD28 beads. As shown **in Table 2**, peak expression measured by flow cytometric analysis varied between the different immunomodulators; however, the majority of them reached maximal levels of display after 96 hours of stimulation. After 96 hours of stimulation, all IC were well expressed in more than 50% of the gated population except BTLA, which reached a maximum of display in 40% of the population, and TIGIT, which only slightly increased its expression levels. Similar results were obtained by repeating the same treatment on the same hPBMC sample and on hPBMCs from different donors (not shown). In order to clarify the determination of expression (%) of each target on human lymphocytes, reported in **Table 2**, as well as gating strategy, representative fluorescence-activated cell sorting (FACS) analyses of the time course of activation for the indicated immune checkpoints on human lymphocytes have been reported **in Figure 15**. On the basis of this analysis, we have chosen 96 hours as the time point for the activation of lymphocytes to be used for the selection of the human scFv library. The strategy of using activated lymphocytes in the first panning was devised to ensure targeting of proteins with their native conformation, as that presented on the cell membrane, and to obtain a productive enrichment of several phage clones against multiple targets in one single shot, thus reducing also the time requested for multiple parallel selections.

To this aim about one million phage particles were selected by panning the library ($1 \cdot 10^{12}$ different phages) on activated hPBMCs as described in the Materials and Methods section (selection cycle 1). A

negative panning on untreated lymphocytes was performed for some selections to remove from the repertoire all the non-specific phages that recognize common antigens on the cell surface (see Materials and Methods). For the isolation of scFvs against some targets also expressed at similar levels on untreated lymphocytes, such as CD27, BTLA and TIGIT, the negative panning was not carried out to avoid the loss of some specific phages in the subtractive selection.

The pool of phages obtained from cycle 1 potentially represented a large collection of binders to many different IC, henceforth referred to as the 'Immunome Library'. To facilitate the identification of molecules recognizing specific receptors, we used a panel of 10 recombinant proteins to further affinity select the Immunome Library. With the aim of developing a universal protocol for the selection of antibodies to cell surface displayed proteins, we performed 10 different parallel selections with two subsequent cycles of selection on recombinant Fc-fusion proteins. This strategy represented a compromise between efficiency of selection and generation of IC-specific repertoires with significant diversity to allow for the identification of antibodies binding to different regions of the target IC and with different biological activities. In parallel, a conventional selection performed by three panning cycles on the purified protein only was carried out for LAG-3/Fc, followed by ELISA in order to do a comparison with the novel proposed approach **(data not shown) (Sasso et al. 2018)**.

Level of expression (%) of each target on human lymphocytes

Immune checkpoints	*Untreated hPBMCs*	*(24h) activated hPBMCs*	*(96h) activated hPBMCs*
TIM-3	*0,8*	*20*	*65*
BTLA	*47*	*33*	*40*
TIGIT	*11*	*17.5*	*24*
OX-40	*2*	*67*	*86*
4-1BB	*1*	*53,5*	*70*
CD-27	*36*	*28*	*60*
ICOS	*3*	*32*	*90*
PD-1	*11*	*52*	*95*
PD-L1	*7*	*90*	*99*
LAG-3	*1*	*53*	*59*

Table 2. Expression profile (% of the positive cells) of each target on human lymphocytes. Percentage of expression was calculated as an average of the fraction of human lymphocytes expressing each target from 8 different donors untreated or activated at different time intervals. Standard Deviations ≤ 10% **(Sasso et al. 2018)**.

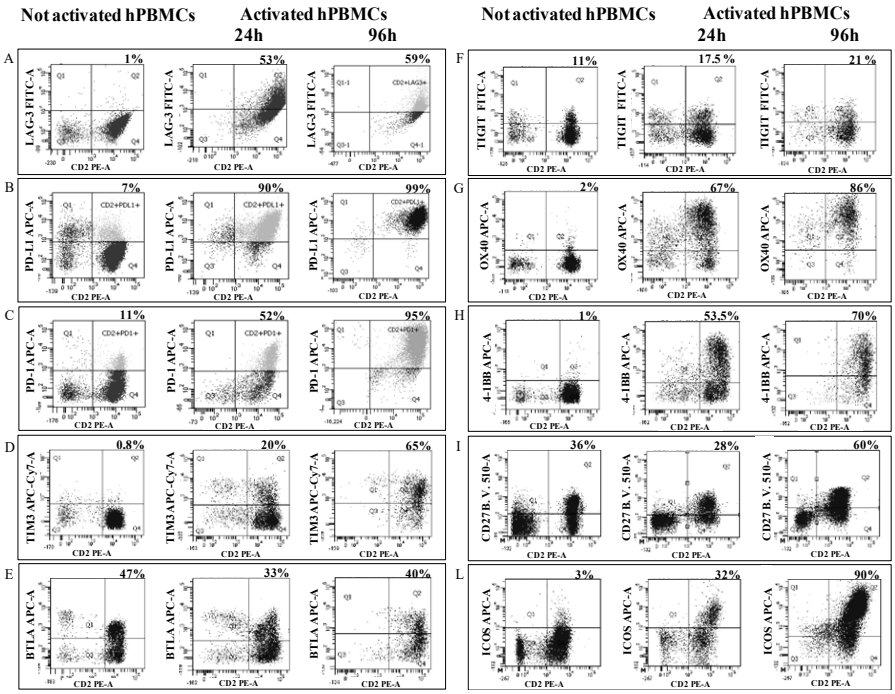

Figure 15. FACS analysis of expression of immunomodulators on human lymphocytes untreated or stimulated for different time intervals. Representative FACS analyses of time course of activation for the indicated immune checkpoints on human lymphocytes. Lymphocytes were identified by analyzing the forward (FSC) versus side (SSC) scatter and gated to exclude debris. The live cells only were considered to measure the percentage of positive cells corresponding to the fraction of double positive population (fluoresence intensity range of 10^2-10^5) for both the expression of CD2 (the T-Lymphocytes lineage marker) and of the specific target of interest: LAG-3 (A), PD-L1 (B), PD-1 (C), TIM3 (D), BTLA (E), TIGIT (F), OX40 (G), 4-1BB (H), CD27 (I) or ICOS (L). Unstained cells or cells treated with the appropriate isotype control were used as background control **(Sasso et al. 2018)**.

2.2 Identification of enriched scFv sequences by next-generation sequencing and conversion into mAbs

To identify individual phage clones selected by the combined ex vivo/*in vitro* approach, we decided to sequence the VH regions of

the IC-specific repertoires by massive parallel sequencing on the MiSeq Illumina platform (see Methods Section for details). To this aim, DNA from each repertoire of each selection cycle was extracted and then digested with suitable restriction enzymes to extract the inserts encoding scFvs. High-throughput sequence analyses of the whole set of selections was performed in collaboration with the research group of Professor N. Zambrano from our Department of Molecular Medicine and Medical Biotechnology.

As a proof of concept of the quality/potency of the binders identified by this novel approach, the scFv sequences that were specifically enriched after panning on three targets, i.e., LAG-3, PD-1 and PD-L1, were chosen for further studies. Indeed, antibodies specific for two of these targets, such as anti-PD-1 Nivolumab and anti-PD-L1 Atezolizumab, have been previously developed and widely used in the clinic, and thus they can be used for comparison in biological assays. Starting from the most enriched sequences for each of the LAG-3, PD-1 and PD-L1 IC-specific repertories, we accomplished the rescue of the corresponding scFvs (as described in Methods). The conversion of scFvs into more stable antibody formats (IgG4 isotype) was carried out by subcloning the variable regions into two eukaryotic vectors for the expression of H and L chains and by transfecting the resulting recombinant vectors into HEK293-EBNA cells. This task was carried out in collaboration with the research group of Professor N. Zambrano **(Sasso et al. 2018)**.

2.3 Human IgGs generated from selected binders show high binding affinity and receptor/ligand competitive activity

Human IgG4 antibodies generated from the best ranking LAG-3, PD-1 and PD-L1 binders were confirmed to recognize human activated PBMCs and recombinant proteins with low nanomolar or sub-nanomolar affinity (**see Figure 16, Table therein, and Figure 17**). In particular, some anti-PD-1 mAbs (i.e., PD-1_1 and PD-1_2) showed comparable or higher apparent affinity compared to the clinically validated Nivolumab. Most of the anti-PD-1 and anti-PD-L1 antibodies, including Nivolumab, displayed similar binding to the recombinant protein compared to the activated hPBMCs, while the

anti-LAG-3 antibodies showed higher affinity for the activated hPBMCs. Two or three of the original five antibodies chosen were used for further characterization because they were highly specific for both recombinant targets and activated lymphocytes, whereas they showed no or poor binding to Fc or untreated lymphocytes **(see Figure 16 and 17)**. The other IgG4 were discarded because they recognized the Fc or not activated lymphocytes (data not shown). As for the anti-LAG-3 scFvs selected by the conventional strategy on purified recombinant protein only and screened by ELISA assays, only a low percentage (15%) of positive clones contained a cDNA sequence encoding the whole scFv (with no stop codons or other rearrangements). The few clones expressing the whole scFvs were converted into human IgG4, and were found to be capable of binding to the purified protein, but they recognized the activated lymphocytes with lower affinity **(data not shown).** Furthermore, some of them were found to be unstable during their storage at 4°C for 2-4 days, thus they were not used for further characterization.

Because anti-PD-L1 antibodies have been shown to provide for clinical benefit by blocking interaction between PD-L1 expressed on cancer cells and PD-1 displayed by T cells **(Shultz 2017)**, we tested whether the anti-PD-L1 antibodies would also recognize their targets on the surface of cancer cells. All anti-PD-L1 antibodies showed high affinity for tumor cells expressing PD-L1, such as mammary MDA-MB-231 tumor cells, and the hierarchy of binding activity to tumor cells was similar to that observed with activated hPBMCs **(Figure 16 and Table therein) (Sasso et al. 2018)**.

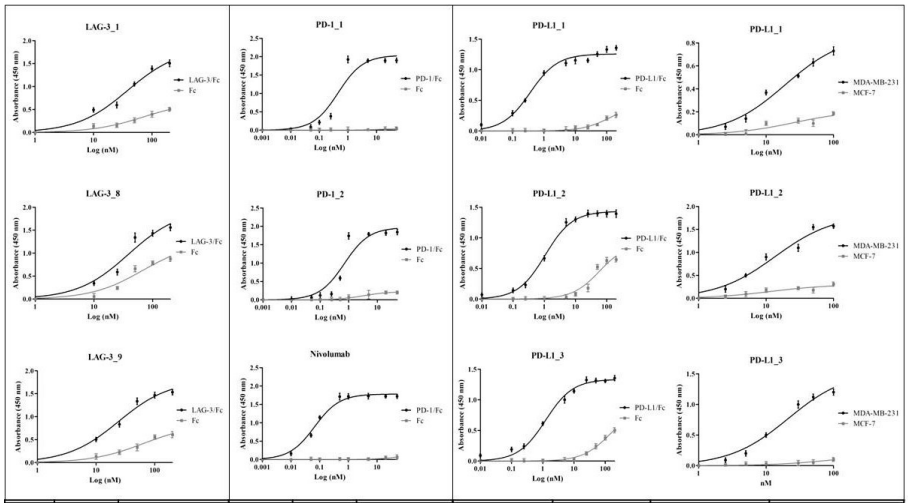

	LAG-3/Fc	Activated hPBMCs		PD-1/Fc	Activated hPBMCs		PD-L1/Fc	Activated hPBMCs	MDA-MB-231 cells
LAG-3_1	38 nM	6 nM	PD-1_1	0,4 nM	0,14 nM	PD-L1_1	0,3 nM	9 nM	19 nM
LAG-3_8	52 nM	9 nM	PD-1_2	0,7 nM	0,9 nM	PD-L1_2	1 nM	0,4 nM	13 nM
LAG-3_9	24 nM	19 nM	Nivolumab	0,066 nM	0,4 nM	PD-L1_3	1,2 nM	16 nM	21 nM

Figure 16. Binding of the selected antibodies to the purified recombinant proteins and tumor cells. Binding curves of the antibodies to each target protein/Fc (black curves) or Fc (grey curves) are reported in the left and central panels. The binding curves of the anti-PD-L1 mAbs to MDAMB231 cells (black curves) or MCF-7 cells (grey curves) are reported in the right panel. The Kd values obtained from the binding curves of the antibodies to each target protein/Fc, activated hPBMCs and tumor cells are reported in the table. Binding values were reported as the mean of at least three determinations obtained in three independent experiments. Error bars depicted means ± SD. **(Sasso et al. 2018).**

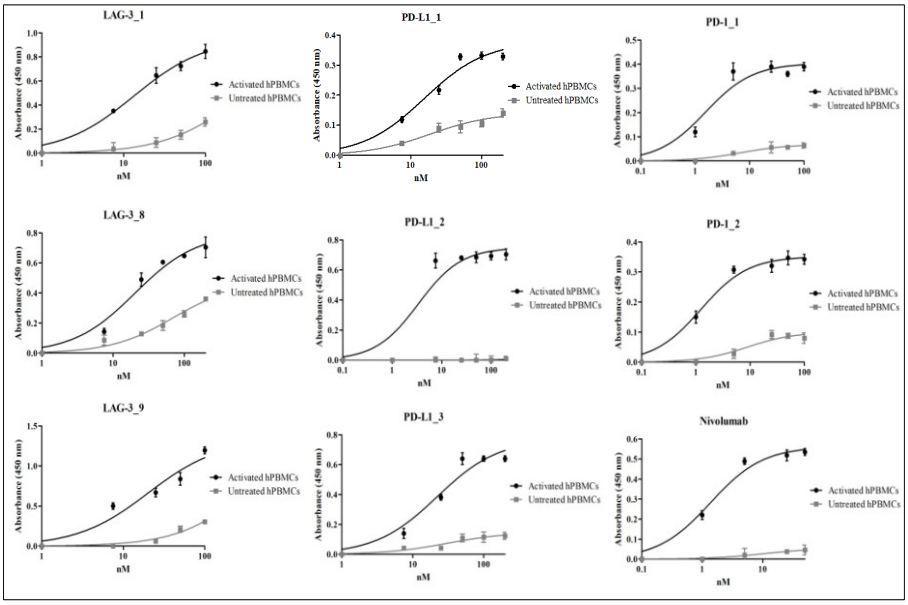

Figure 17. Binding affinity of the selected antibodies for lymphocytes. The ELISA assays were performed with the anti-PD-1, anti-PD-L1 and anti-LAG-3 mAbs (obtained after the three cycles of selection) used at increasing concentrations (7.5 nM, 25 nM, 50 nM, 100 nM) on activated hPBMCs (black curves) or untreated hPBMCs (grey curves). Binding values were reported as the mean of at least three determinations obtained in three independent experiments. Error bars depicted means ± SD. **(Sasso et al. 2018)**.

2.4 High affinity IgGs against immune checkpoint molecules display T cell immunostimulatory activity

Previous reports showed that CD3-positive primary resting cells in unfractionated hPBMCs can be induced to proliferate *in vitro* by using Staphylococcal enterotoxin B (SEB) or (phytohemagglutinin (PHA), and that this activity is modulated by CI **(Selby et al 2016; Wang et al. 2014; Maçon-Lemaître and Triebel 2005).** We therefore used this assay to test whether the selected antibodies against LAG-3, PD-1 or PD-L1 were able to increase cell division. To this end, some mAbs among those with the highest affinity and specificity were tested for their biological activity in a flow

cytometry-based lymphocyte proliferation assay that allows identification of proliferating T cells by anti-CD3 staining.

With this aim, CFDA-SE-stained lymphocytes were stimulated with PHA, and incubated in the absence or presence of the antibodies to induce T cell proliferation. In this assay, Nivolumab consistently led to a 50% increase in proliferative activity and the anti-PD-1 antibodies PD-1_1 and PD-1_2 were also able to efficiently stimulate T cell proliferation with the former showing higher activity than Nivolumab **(Figure 18A).** Similarly, all three antibodies against PD-L1 and one of the three LAG-3 antibodies also induced various degrees of proliferation. The ability to stimulate proliferation did not always correlate with the binding potency, suggesting that the different antibodies may have distinct modes of interactions with their targets. The antibodies PD-1_1 and PD-L1_1 that were the best activating antibodies on human lymphocytes confirmed this ability also on murine lymphocytes **(Figure 19)**, thus suggesting that they are cross-reactive with mouse PD-1 and PD-L1.

We used MDA-MB-231 breast tumor cells, which express high levels of PD-L1 on their surface, to test the ability of the anti-PD-L1 and anti-PD-1 antibodies to suppress the inhibitory action of the PD-1/PD-L1 interaction on lymphocyte proliferation when the two cell types are co-cultured. As shown **in Figure 18B,** mAbs PD-L1_1 and PD-1_1 induced the proliferation of lymphocytes in a dose-dependent manner, whereas only a slight effect was detected on lymphocytes treated with mAbs PD-L1_2 and PD-1_2 **(data not shown).** Also in this assay mAbs PD-L1_1 and PD-1_1 displayed higher activity than Nivolumab, while no effects on the proliferation of lymphocytes were observed when PD-L1-negative MCF-7 tumor cells were used. In competition ELISA assays, we showed that mAbs PD-L1_1 and PD-L1_2 were able to interfere with the recognition of PD-L1 by its two receptors PD-1 and B7.1 **(Figure 20)**.

However, we suppose that these novel antibodies could act not only by interfering in PD-1 and PD-L1 interaction, but also by other antagonistic effects on their receptors or ligands. Indeed, it is likely that PD-1_1 has a different mechanism of action with respect to that of Nivolumab. This hypothesis is based on the results obtained by competitive ELISA assays, performed by measuring the binding to immobilized PD-1 of biotinylated Nivolumab in the absence or in the presence of saturating concentrations of unlabelled PD-1_1 and PD-

1_2 mAbs. As shown in **Figure 21**, the binding curves of biotinylated Nivolumab in the absence or in the presence of PD-1_1 or PD-1_2 mAbs are superimposable, thus suggesting that the novel PD-1_1 and PD-1_2 mAbs do not interfere with Nivolumab in the interactions with PD-1 receptor **(Sasso et al. 2018)**.

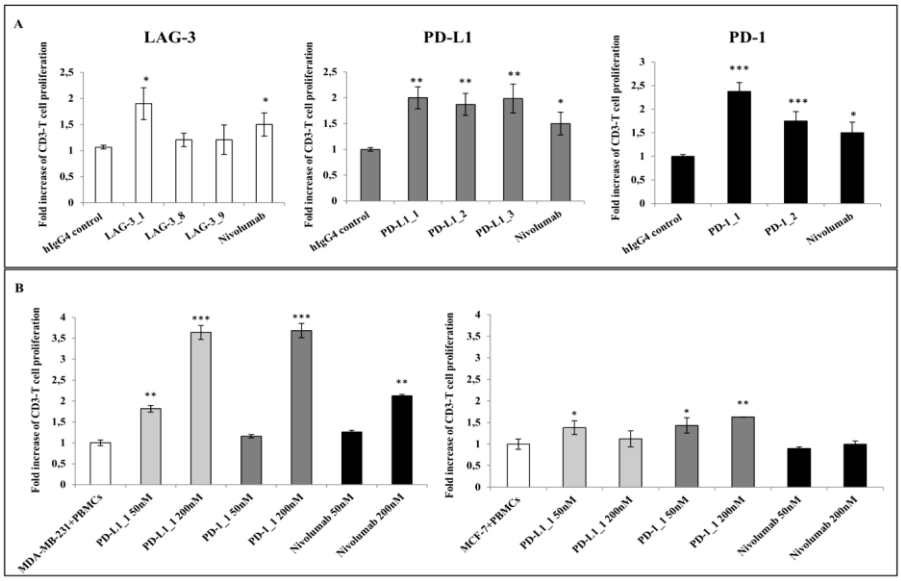

Figure 18. Effects of the novel antibodies on lymphocyte proliferation. A: Proliferation of hPBMCs after stimulation with PHA at 2.5 µg/ml in the absence or in the presence of the immunomodulatory mAbs. Fold increase of $CD3^+$ T cell proliferation determined by the indicated selected antibodies was measured by anti-CD3 staining by FACS with respect to activation of hPBMCs with PHA in the absence of antibodies or in the presence of an unrelated IgG4. B: Effects of anti-PD-L1 antibodies on Lymphocyte proliferation as induced by tumor cells. Fold increase of hPBMCs proliferation as determined by normalized absorbance values obtained by ELISA with anti-BrdU antibodies in hPBMCs samples co-cultured with MDA-MB-231 (left panel) or MCF-7 (right panel) tumor cells in the absence (white bar) or in the presence of increasing concentrations (50 nM and 200 nM) of PD-L1_1 (light grey bars) or PD-1_1 (grey bars) antibodies for 72 hours at 37°C. Nivolumab was used, in both the experiments, as a positive control (black bars). Concentration values were reported as the mean at least three determinations in five independent experiments performed by using lymphocytes from 5-8 healthy donors. Error bars depicted means ± SD. *P* values for the indicated mAbs relative to unrelated IgG4 are: ***$P \leq 0{,}001$; **$P < 0{,}01$; *$P < 0{,}05$ **(Sasso et al. 2018)**.

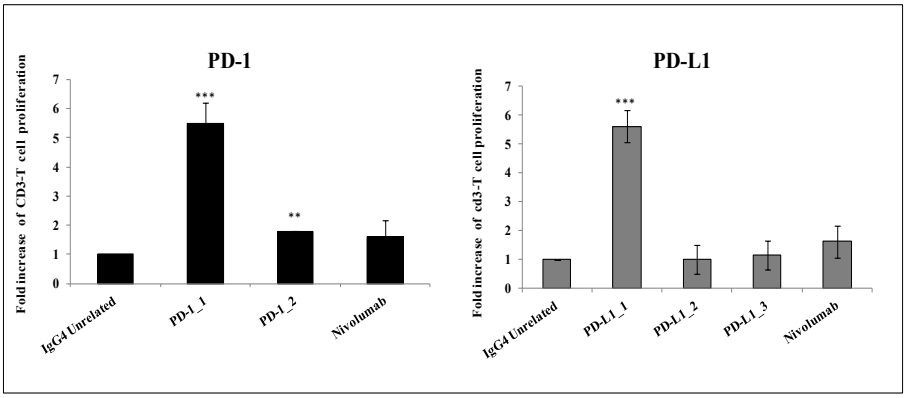

Figure 19. Proliferation of mouse PBMCs after stimulation with PHA at 2.5 µg/ml in the absence or in the presence of the immunomodulatory antibodies. Fold increase of CD3-T cell proliferation determined by the indicated selected antibodies was measured with respect to activation of mouse PBMCs with PHA at 2.5 µg/ml in the absence of antibodies or in the presence of an unrelated IgG4 (10µg/ml). Concentration values were reported as the mean at least three determinations in five independent experiments performed by using lymphocytes from 5-8 healthy donors. Error bars depicted means ± SD. *P* values for the indicated mAbs relative to unrelated IgG4 are: ***$P \leq 0.001$; **$P < 0.01$ **(Sasso et al. 2018)**.

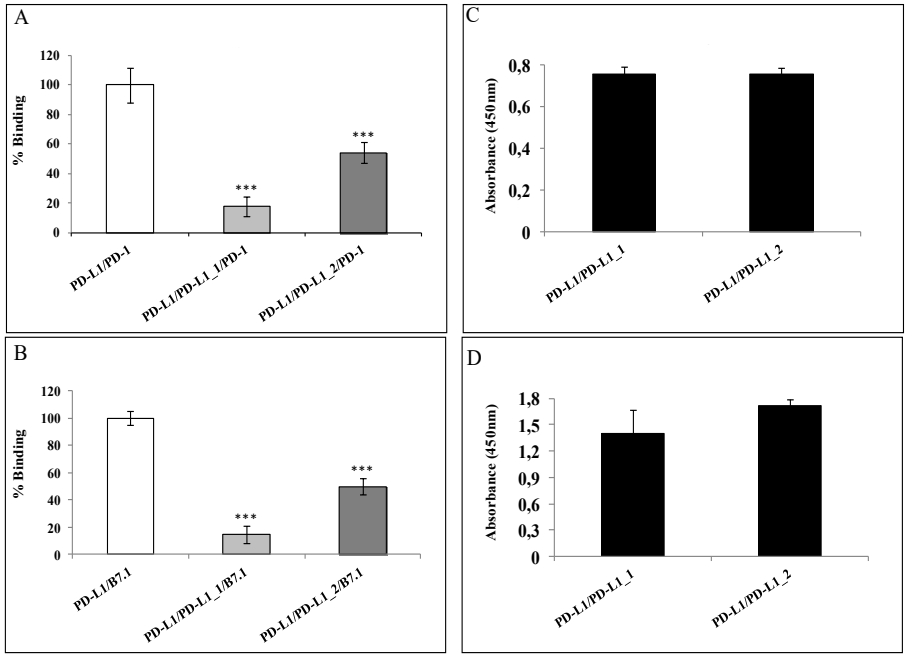

Figure 20. Competitive binding assays. Competitive ELISA assays were performed by testing the binding of the biotinylated chimeric proteins PD-1/Fc (panel A) or B7.1/Fc (panel B) to PD-L1 in the absence (white bars) or in the presence of the unlabeled competitive PD-L1_1 and PD-L1_2 antibodies (grey bars). In both the experiments the binding of the novel PD-L1_1 and PD-L1_2 antibodies to PD-L1 chimeric protein was tested as a control in parallel assay (panels C and D). Binding values were reported as the mean of at least three determinations obtained in three independent experiments. Error bars depicted means ± SD. *P* values for the indicated mAbs relative to control are: ***$P \leq 0.001$ **(Sasso et al. 2018)**.

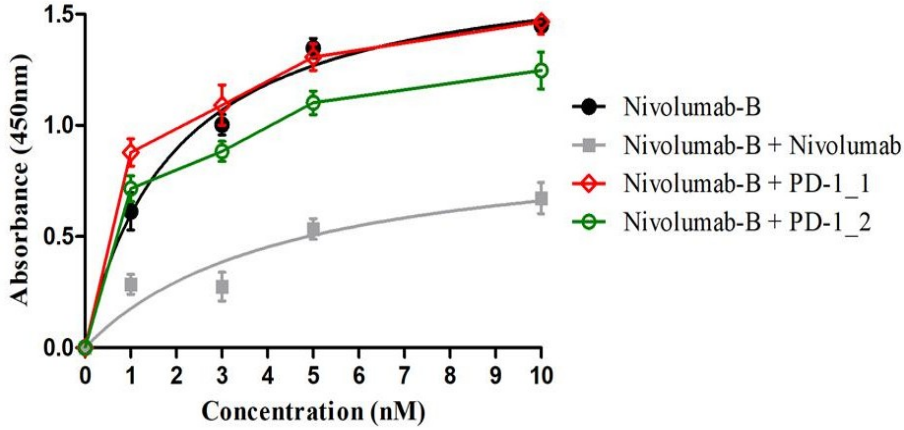

Figure 21. Competitive ELISA assay of PD-1_1 or PD-1_2 mAbs with biotinylated Nivolumab (Nivolumab-B). Competitive ELISA assays were performed by measuring the binding of Nivolumab-B to PD-1 at the indicated concentrations (1, 3, 5 and 10nM) in the absence (black curve) or in the presence of the unlabeled PD-1_1 (red curve) or PD-1_2 (green curve) mAbs used at saturating concentration (400nM), respectively. In a parallel assay, the binding of Nivolumab-B was tested in the presence of the unlabeled Nivolumab (grey curve) at the same saturating concentration. Binding values were reported as the mean of at least three determinations obtained in three independent experiments. Error bars depicted means ± SD.

2.5 Effects of the novel high affinity IgGs against immune checkpoint molecules on secretion of cytokines

Immunomodulatory antibodies, such as Nivolumab, Ipilimumab and Pembrolizumab were shown to improve T cell effector functions, with this property potentially increasing their clinical benefit **(Maçon-Lemaître and Triebel 2005; Wang et al. 2014; Selby et al. 2016).**

We therefore tested five antibodies among those with the highest ability to induce T cell proliferation (LAG-3_1, PD-1_1, PD-1_2, PD-L1_1, and PD-L1_2) in a cytokine secretion **(Sanmamed et al. 2015)** assay previously reported for the characterization of Nivolumab **(Wang et al. 2014)**. In this assay, we included Atezolizumab as an additional positive control **(Patel et al. 2017;**

Shultz 2017). As shown in **Figure 22**, all the tested antibodies were able to increase the secretion of both IL-2 and interferon IFNγ by hPBMCs stimulated with either PHA or SEB. Cytokine secretion increased over time upon addition of the different antibodies to the cell culture mixture. PD-1_1 mAb appeared to be consistently more potent than all the other tested antibodies for its ability to stimulate secretion of both cytokines. Also, in this assay most of the newly identified antibodies compared well with Nivolumab and Atezolizumab, further supporting the conclusion that the Immunome Library that we generated is enriched in binders with good potential for being developed for clinical use **(Sasso et al. 2018)**.

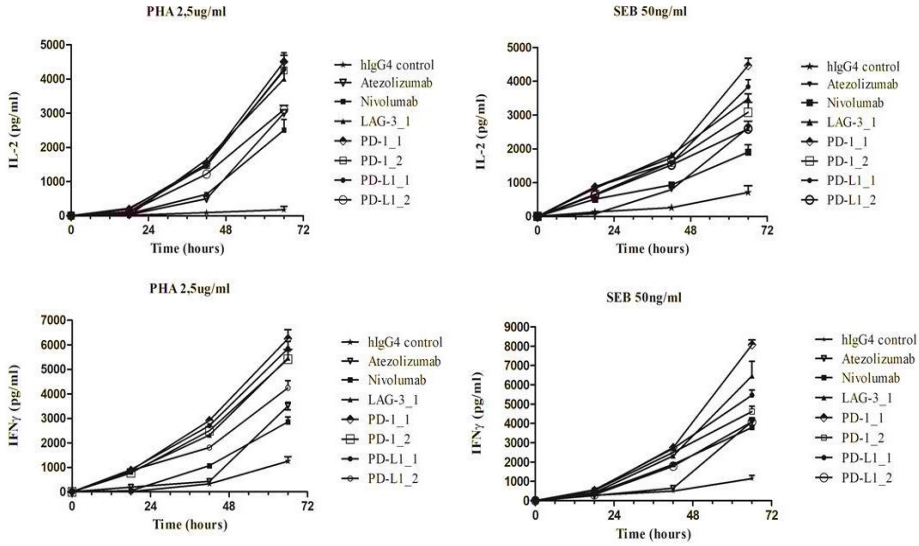

Figure 22. Effects of the novel immunomodulatory antibodies on secretion of cytokines by stimulated T cells. IL-2 and IFNγ values obtained by ELISA assays on supernatants of hPBMCs stimulated with PHA (2.5 µg/mL) or SEB (50 ng/mL) in the absence or in the presence of the antibodies LAG-3_1, PD-1_1, PD-1_2, PD-L1_1, PD-L1_2 at the concentration of 20µg/ml for 18-66 hours at 37°C. Nivolumab, Atezolizumab and an unrelated antibody were used as a positive and negative control, respectively. Concentration values were reported as the mean at least three determinations in five independent experiments performed by using lymphocytes from 5-8 healthy donors. Error bars depicted means ± SD **(Sasso et al. 2018)**.

2.6 In vivo antitumor activity

The two antibodies PD-1_1 and PD-L1_1, given their cross-reactivity with mouse PD-1 and PDL1, were also tested *in vivo* on the CT26 colon cancer model in collaboration with the research group of Professor A. Nicosia from our Department of Molecular Medicine and Medical Biotechnology. Mice were implanted with CT26 cells (day 0) and then treated with PD-1_1 and PD-L1_1 antibodies (day 3, 6, 10). Two commercially available antibodies reacting against murine PD-1 and PD-L1 (α-mPD-1 and α-mPD-L1), and previously validated *in vivo*, were used as positive controls **(Wang et al. 2016)**. While the growth rate of tumors in untreated mice was very fast and uncontrolled, with the majority of tumors reaching sizes of > 650 mm^3 at day 21, a reduction in tumor volume was found in mice treated with PD-1_1 ($p=0.03$). The activity of the cross-reactive anti-PD-1 antibody is comparable to that of the commercial antibody against murine PD-1. A trend of comparable activity was also observed for the two anti-PD-L1 antibodies **(Figure 23)**. Treated mice consistently show a dichotomy in the response to PD-1 and PD-L1 blockade with two distinct treatment outcomes, responder and non-responder mice, as well described for this and other cancer models. During the period of treatment, the animals did not show signs of wasting or other visible signs of toxicity. Thus, the biological and functional activity of the two novel mAbs was also confirmed in a relevant *in vivo* model **(Sasso et al. 2018)**.

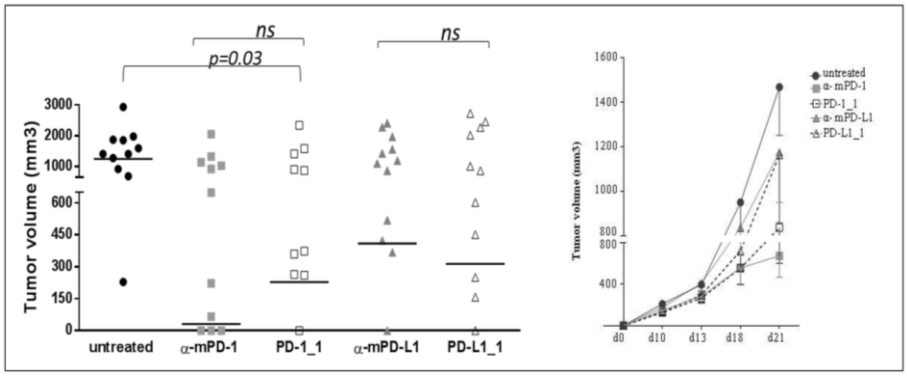

Figure 23. ***In vivo*** **antitumor activities of PD-1_1 and PD-L1_1 antibodies**. Tumor growth in groups of 10-12 mice inoculated with CT26 cells at day 0 and treated with PD-1_1, PD-L1_1 or positive control antibodies reacting against murine PD-1 and PD-L1 (α-mPD-1, α-mPD-L1) at day 3, 6 and 10. Shown is tumor volume for individual mice at day 21 (left) and mean of tumor volume for each group over time (right panel) **(Sasso et al. 2018)**.

DISCUSSION AND CONCLUSIONS

During the past three decades, anticancer immunotherapy has evolved as an encouraging therapeutic option and a number of immunotherapeutic drugs have been approved by the FDA for clinical use. Furthermore, many innovative therapeutic regimes, involving the combination of new drugs with conventional treatments, are being designed and tested in clinical trials with promising results **(Galluzzi et al. 2014)**.

Tumor-targeting monoclonal antibodies, endowed with intrinsic antineoplastic activity, belong to the passive form of immunotherapy, whereas antibodies targeting immune regulatory checkpoints, employing anticancer effects only upon the engagement of the host immune system, belong to the active form of immunotherapy **(Galluzzi et al. 2014; Papaioannou et al. 2016)**.

1. Immunotherapy based on novel human immunoagents specific for TAAs

The current trends for the use of antibodies in oncology are to employ them alone or in combinations as therapeutic agents. The specific and direct inhibition of the signal transduction of receptors, expressed on tumor cells **(Wurz et al. 2016)** and involved in tumor cell survival and proliferation, with a combination of antibodies against distinct noncompeting epitopes is a strategy widely tested **(Riccio et al. 2017)**.

ErbB2 overexpressed in breast cancer and in many other carcinomas represents an attractive target for immunotherapy **(Slamon et al. 1989; Tagliabue et al. 1991; Lohrisch and Piccart 2001; Gravalos and Jimeno 2008)**, and Trastuzumab was the first humanized monoclonal antibody to become standard of care for metastatic ErbB2-positive breast cancer **(Riccio et al. 2017)**. However, some ErbB2-positive tumors are resistant to Trastuzumab,

thus another humanized anti-ErbB2 antibody, named Pertuzumab, has been recently approved by FDA. Since they have different mechanisms of action, as they bind to the domain II and the domain IV of ErbB2 respectively, they can be combined showing superior antitumor activity compared to single agent treatments **(Sabatier and Gonçalves 2014; Stebbing et al. 2000; Romond et al. 2005; Baselga and Swain 2010)**. These findings led to the preclinical evaluation of cocktails of noncompeting antibodies **(Riccio et al. 2017)**, but an important limit was still represented by the increasing cost of treatment.

Furthermore, recently in literature a triparatopic construct targeting EGFR has been reported, which showed superior activity with respect to combination of noncompetitive antibodies, mainly attributed to better matrix induction and increased degradation of EGFR **(Riccio et al. 2017)**. On the basis of these observations, we decided to characterize for the first time a triparatopic immunoagent targeting ErbB2/HER2. To this aim a Tribody format, obtained by genetic fusion of the genes for either the Fab Fd-chain or L chain with the genes of 2 distinct scfv molecules, was used. The trispecific Tribody is an antibody construct (100 kDa) with a lower molecular size than a whole IgG and well suited for both tumor penetration and acceptable half-life **(Riccio et al 2017)**. The Tribody, named TbTPE, was designed to contain three binding sites recognizing three distinct non-overlapping epitopes of ErbB2, derived from Erb-hcAb, Pertuzumab and Trastuzumab. We show here that the triparatopic Tribody TPE is able to bind to all the ErbB2-positive tumor cells tested, to downregulate ErbB2 on ErbB2-positive tumor cells, and to inhibit tumor growth more efficiently than the trivalent monoparatopic controls (Tb-TTT, Tb-PPP, Tb-EEE), or compared with a combination of 3 different bivalent monoparatope monoclonal antibodies, recognizing different epitopes of the receptor. Interestingly, the multiparatope Tribody Tb-TPE is able to affect also the growth of Trastuzumab-resistant tumor cells, such as the MCF7-HER2Δ16 or JIMT-1 cells, by dramatically reducing the level of ErbB2, thus providing a useful tool to overcome resistance.

This novel construct has the following advantages: it combines in 1 single molecule 3 different targeting approaches and antitumor actions of 3 different antibodies, such as Trastuzumab, Pertuzumab and Erb-hcAb; it can be used for a larger patient population due to its

ability to overcome the tumor heterogeneity; it allows to reduce the costs of antibody production as only 1 construct provides the effects of 3 different antibodies.

2. Immunotherapy based on immunomodulatory mAbs

The other antibody-based approach in oncology is represented by the immunomodulatory mAbs that operate by interacting with soluble or cellular components of the immune system, to elicit a novel, or prolong an existing anticancer immune response **(Galluzzi et al. 2014; Peggs et al. 2009)**. The first mAbs recently approved by FDA for this approach include three classes of immune checkpoint-blocking mAbs for clinical treatment of a variety of solid tumors: Ipilimumab (anti-CTLA4 mAb), Pembrolizumab and Nivolumab (anti-PD-1 mAbs) and Atezolizumab, Durvalumab and Avelumab (anti-PD-L1 mAbs) **(Galluzzi et al. 2014; Brahmer et al. 2012; Patel et al 2017; Shultz 2017; Callahan et al. 2016)**. However, the efficacy of these checkpoint inhibitors is still limited to 20–30% of the population, and could not be shown in highly prevalent cancer types **(Lee et al. 2013; Pardoll 2012; Buqué et al. 2015; Anderson et al. 2016).** Interestingly, the combination of anti-PD-1 and anti-CTLA-4 antibodies, resulted in a longer higher rate of response with respect to that observed with the single mAb treatments in metastatic melanoma and MSI-associated colorectal cancer **(Mahoney et al. 2015; Larkin et al. 2015)**, thus indicating that proper combination of different antibodies could be essential to achieve a more effective immune-based cancer therapy. Thus, further progress in the field could be represented by the generation of a complete repertoire of fully human antibodies specific for many immune checkpoints to be tested, either alone or in appropriate combinations for rapid translation into the clinic **(Sasso et al . 2018)**.

With this aim, a novel selection strategy by phage display on live hPBMCs was performed to obtain an unbiased library of immune checkpoint binders. This strategy consisted in a negative panning on untreated hPBMCs to remove all the non-specific binders, followed by a positive panning on activated hPBMCs to collect only the scFvs specifically binding to receptors expressed on activated lymphocytes.

For the following identification of the clones specific for each target, we combined the *ex vivo/in vitro* selection with the Next-Generation Sequencing approach for a more rapid and efficient selection with respect to the conventional strategy, carried out by panning on the purified protein only and followed by screening with ELISA assays. Using this novel strategy, we rapidly identified more stable human IgG4 antibodies, endowed with biological activity, and able to recognize the cell-displayed receptors with apparent affinity in the low nanomolar range and down to 0,1–0,4 nM. This binding affinity is well within what has already been shown with clinically active checkpoint-specific antibodies, and compares well with that of the clinically approved Nivolumab **(Sasso et al. 2018)**.

As a proof of concept in this thesis work we further characterized the antibodies specific for PD-1, PD-L1 and LAG-3. The choice of these three targets was based on the observation that selections on them gave rise to median levels of enrichment, and on the availability of antibodies specific for two of these targets to be used for comparison in well established *in vitro* assays to evaluate their functional activity. From the list of the top 10 ranking scFv sequences, at least 5 effective antibodies for each of these three targets were converted into IgG4 and found to be expressed at satisfactory levels, stable in solution and capable of binding to their targets. Overall, as indicated in the results, from the total converted IgGs eleven of them displayed low nanomolar apparent affinity for their cognate receptor expressed on hPBMCs, with PD-L1_2, PD-1_1 and PD-1_2 mAbs endowed with a sub-nanomolar apparent affinity comparable to that of Nivolumab.

Among them, at least 2–3 of the 5 converted antibodies for each target were found to be highly specific for both recombinant purified targets and activated lymphocytes, with no significant binding to untreated lymphocytes or Fc, and thus they were chosen for further biological and functional assays. When tested for their ability to stimulate T cell proliferation LAG-3_1, PD-L1_1, PD-L1_2, PD-L1_3, PD-1_1 and PD-1_2 mAbs did show biological activity and in particular the PD1_1 mAb was found to perform better than the clinically approved Nivolumab. PD-1_1 also displayed significant activity in promoting T cell proliferation in co-cultures with high PD-L1-expressing tumor cell line MDA-MB-231. In this assay also the PD-L1_1 mAb almost tripled T cell proliferation, consistently with its

ability to interfere with PD-L1/PD-1 interaction. We further demonstrated that some of the selected antibodies can stimulate T cells to secrete IL-2 and IFNγ, confirming the observation that some of the antibodies identified in this work display binding affinities and biological properties similar to the clinically validated Atezolizumab and Nivolumab **(Wang et al. 2014; Wang et al. 2016; Selby et al. 2016)**. Due to the property of PD-1_1 and PD-L1_1 mAbs to cross-react with mouse lymphocytes, differently from Nivolumab, they were tested *in vivo* and found to efficiently inhibit tumor growth without apparent toxic effects on mice bearing CT26 colon carcinoma **(Sasso et al . 2018)**.

Further studies are needed to carefully monitor auto-immune side effects, potentially induced by these antibodies, however, due to their high affinity; they could allow to reduce the therapeutic doses and the consequent eventual unwanted side effects. Moreover, the data presented in this work support the conclusion that our selection procedure allows for the generation of antibodies specifically recognizing their target receptor in its native conformation and with high affinity without need for further affinity maturation.

Furthermore, considering the ability of the novel identified antibodies to stimulate T cell proliferation and display effector functions in a manner comparable to, or even superior than, Nivolumab, which has shown clinical activity in different type of cancer diseases, this study suggests that the 'Immunome Library' generated in this project is enriched in binders with good potential for being developed for clinical use.

REFERENCES

Ahmad ZA, Yeap SK, Ali AM, Ho WY, Alitheen NB, Hamid M. 2012. scFv antibody: principles and clinical application. Clin Dev Immunol. 2012:980250.

Amer Assal, Justin Kaner, Gopichand Pendurti, Xingxing Zang. 2015. Emerging targets in cancer immunotherapy: beyond CTLA-4 and PD-1. Immunotherapy. 7(11): 1169–1186.

Anderson AC, Joller N, Kuchroo VK. 2016. Lag-3, Tim-3, and TIGIT: Co-inhibitory Receptors with Specialized Functions in Immune Regulation. Immunity. 44(5):989-1004.

Barnhart C. 2015. Pembrolizumab: First in Class for Treatment of Metastatic Melanoma. J Adv Pract Oncol. 6(3):234-8.

Baselga J, Swain SM. 2009. Novel anticancer targets: revisiting ERBB2 and discovering ERBB3. Nat Rev Cancer. 9(7):463-75.

Baselga J, Swain SM. 2010. CLEOPATRA: a phase III evaluation of pertuzumab and trastuzumab for HER2-positive metastatic breast cancer. Clin Breast Cancer. 10(6):489-91.

Bazan J, Całkosiński I, Gamian A. 2012. Phage display--a powerful technique for immunotherapy: 1. Introduction and potential of therapeutic applications. Hum Vaccin Immunother. 8(12):1817-28.

Brahmer JR, Tykodi SS, Chow LQ, Hwu WJ, Topalian SL, Hwu P, Drake CG, Camacho LH, Kauh J, Odunsi K et al. 2012. Safety and activity of anti-PD-L1 antibody in patients with advanced cancer. N Engl J Med. 366(26):2455-65.

Buqué A, Bloy N, Aranda F, Castoldi F, Eggermont A, Cremer I, Fridman WH, Fucikova J, Galon J, Marabelle A et al. 2015. Trial Watch: Immunomodulatory monoclonal antibodies for oncological indications. Oncoimmunol. 4(4):e1008814.

Burugu S, Gao D, Leung S, Chia SK, Nielsen TO. 2017. LAG-3+ tumor infiltrating lymphocytes in breast cancer: clinical correlates and association with PD-1/PD-L1+ tumors. Ann Oncol. 28(12):2977-2984.

Busse D, Doughty RS, Arteaga CL. 2000. HER-2/neu (erbB-2) and the cell cycle. Semin Oncol. 27(6 Suppl 11):3-8.

Callahan MK, Flaherty CR, Postow MA. 2016. Checkpoint Blockade for the Treatment of Advanced Melanoma. Cancer Treat Res. 167:231-50.

Camorani S, Esposito CL, Rienzo A, Catuogno S, Iaboni M, Condorelli G, de Franciscis V, Cerchia L. 2014. Inhibition of receptor signaling and of glioblastoma-derived tumor growth by a novel PDGFRβ aptamer. Mol Ther. 22(4):828-41.

Camorani S, Cerchia L. 2015. Oligonucleotide aptamers for glioma targeting: an update. Cent Nerv Syst Agents Med Chem. 15(2):126-37.

Camorani S, Crescenzi E, Colecchia D, Carpentieri A, Amoresano A, Fedele M, Chiariello M, Cerchia L. 2015. Aptamer targeting EGFRvIII mutant hampers its constitutive autophosphorylation and affects migration, invasion and proliferation of glioblastoma cells. Oncotarget. 6(35):37570-87.

Camorani S, Crescenzi E, Gramanzini M, Fedele M, Zannetti A, Cerchia L. 2017. Aptamer-mediated impairment of EGFR-integrin αvβ3 complex inhibits vasculogenic mimicry and growth of triple-negative breast cancers. Sci Rep. 7:46659.

Carter P, Presta L, Gorman CM, Ridgway JB, Henner D, Wong WL, Rowland AM, Kotts C, Carver ME, Shepard HM. 1992. Humanization of an anti-p185HER2 antibody for human cancer therapy. Proc Natl Acad Sci U S A. 89(10):4285-9.

Camorani S, Crescenzi E, Fedele M, Cerchia L. 2018. Oligonucleotide aptamers against tyrosine kinase receptors: Prospect

for anticancer applications. Biochim Biophys Acta Rev Cancer. 1869(2):263-277.

Chen L, Flies DB. 2013. Molecular mechanisms of T cell co-stimulation and co-inhibition. Nat Rev Immunol. 13(4):227-42.

Clinicaltrials.gov identifier: nct02061761. 2018. Safety Study of Anti-LAG-3 in Relapsed or Refractory Hematologic Malignancies.

ClinicalTrials.gov Identifier: NCT02966548. 2018. Safety Study of BMS-986016 With or Without Nivolumab in Patients With Advanced Solid Tumors.

ClinicalTrials.gov Identifier:NCT03125928. 2018. Clinical Trial of Atezolizumab With Paclitaxel, Trastuzumab, and Pertuzumab in Patients With Metastatic HER-2 Positive Breast Cancer.

Corraliza-Gorjón I, Somovilla-Crespo B, Santamaria S, Garcia-Sanz JA, Kremer L. 2017. New Strategies Using Antibody Combinations to Increase Cancer Treatment Effectiveness. Front Immunol. 8:1804.

Davis MM, Bjorkman PJ. 1988. T-cell antigen receptor genes and T-cell recognition. Nature. 334(6181):395-402.

De Lorenzo C, Palmer DB, Piccoli R, Ritter MA, D'Alessio G. 2002. A new human antitumor immunoreagent specific for ErbB2. Clin Cancer Res. 8(6):1710-9.

De Lorenzo C, Tedesco A, Terrazzano G, Cozzolino R, Laccetti P, Piccoli R, D'Alessio G. 2004. A human, compact, fully functional anti-ErbB2 antibody as a novel antitumour agent. Br J Cancer. 91(6):1200-4.

De Lorenzo C, Cozzolino R, Carpentieri A, Pucci P, Laccetti P, D'Alessio G. 2005. Biological properties of a human compact anti-ErbB2 antibody. Carcinogenesis. 26(11):1890-5.

De Lorenzo C, Paciello R, Riccio G, Rea D, Barbieri A, Coppola C, Maurea N. 2018. Cardiotoxic effects of the novel approved anti-ErbB2 agents and reverse cardioprotective effects of ranolazine. Onco Targets Ther. 11:2241-2250.

de Melo Gagliato D, Cortes J, Curigliano G, Loi S, Denkert C, Perez-Garcia J, Holgado E. 2017. Tumor-infiltrating lymphocytes in Breast Cancer and implications for clinical practice. Biochim Biophys Acta. 1868(2):527-537.

Decker T, Lohmann-Matthes ML. 1988. A quick and simple method for the quantitation of lactate dehydrogenase release in measurements of cellular cytotoxicity and tumor necrosis factor (TNF) activity. J Immunol Methods. 115(1):61-9.

Drebin JA, Link VC, Greene MI. 1988. Monoclonal antibodies reactive with distinct domains of the neu oncogene-encoded p185 molecule exert synergistic anti-tumor effects in vivo. Oncogene. 2(3):273-7.

Esposito CL, Passaro D, Longobardo I, Condorelli G, Marotta P, Affuso A, de Franciscis V, Cerchia L. 2011. A neutralizing RNA aptamer against EGFR causes selective apoptotic cell death. PLoS One. 6(9):e24071.

Fedele C, Riccio G, Malara AE, D'Alessio G, De Lorenzo C. 2012. Mechanisms of cardiotoxicity associated with ErbB2 inhibitors. Breast Cancer Res Treat. 134(2):595-602.

Frenzel A, Schirrmann T, Hust M. 2016. Phage display-derived human antibodies in clinical development and therapy. MAbs. 8(7):1177-1194.

Friedman LM, Rinon A, Schechter B, Lyass L, Lavi S, Bacus SS, Sela M, Yarden Y. 2005. Synergistic down-regulation of receptor tyrosine kinases by combinations of mAbs: implications for cancer immunotherapy. Proc Natl Acad Sci U S A. 102(6):1915-20.

Galluzzi L, Vacchelli E, Bravo-San Pedro JM, Buqué A, Senovilla L, Baracco EE, Bloy N, Castoldi F, Abastado JP, Agostinis P et al. 2014. Classification of current anticancer immunotherapies. Oncotarget. 5(24):12472-508.

Gatalica Z, Snyder C, Maney T, Ghazalpour A, Holterman DA, Xiao N, Overberg P, Rose I, Basu GD, Vranic S et al. 2014. Programmed cell death 1 (PD-1) and its ligand (PD-L1) in common cancers and

their correlation with molecular cancer type. Cancer Epidemiol Biomarkers Prev. 23(12):2965-70.

Global Burden of Disease Cancer Collaboration, Fitzmaurice C, Dicker D, Pain A, Hamavid H, Moradi-Lakeh M, MacIntyre MF, Allen C, Hansen G, Woodbrook R, Wolfe C et al. 2015. The Global Burden of Cancer 2013. JAMA Oncol. 1(4):505-27.

Goldberg MV, Drake CG. 2011. LAG-3 in Cancer Immunotherapy. Curr Top Microbiol Immunol. 344:269-78.

Goldshmit Y, Trangle SS, Kloog Y, Pinkas-Kramarski R. 2014. Interfering with the interaction between ErbB1, nucleolin and Ras as a potential treatment for glioblastoma. Oncotarget. 5(18):8602-13.

Gravalos C, Jimeno A. 2008. HER2 in gastric cancer: a new prognostic factor and a novel therapeutic target. Ann Oncol. (9):1523-9.

Greenall SA, Donoghue JF, Van Sinderen M, Dubljevic V, Budiman S, Devlin M, Street I, Adams TE, Johns TG. 2015. EGFRvIII-mediated transactivation of receptor tyrosine kinases in glioma: mechanism and therapeutic implications. Oncogene. 34(41):5277-87.

Gross G, Waks T, Eshhar Z. 1989. Expression of immunoglobulin-T-cell receptor chimeric molecules as functional receptors with antibody-type specificity. Proc Natl Acad Sci U S A. 86(24):10024-8.

Haile ST, Dalal SP, Clements V, Tamada K, Ostrand-Rosenberg S. 2013. Soluble CD80 restores T cell activation and overcomes tumor cell programmed death ligand 1-mediated immune suppression. J Immunol. 191(5):2829-36.

Hanahan D, Weinberg RA. 2011. Hallmarks of cancer: the next generation. Cell. 144(5):646-74.

Haynes HR, Camelo-Piragua S, Kurian KM. 2014. Prognostic and predictive biomarkers in adult and pediatric gliomas: toward personalized treatment. Front Oncol. 4:47.

Huang CT, Workman CJ, Flies D, Pan X, Marson AL, Zhou G, Hipkiss EL, Ravi S, Kowalski J, Levitsky HI et al. 2004. Role of LAG-3 in regulatory T cells. Immunity. 21(4):503-13.

Janice M. Reichert. 2017. Antibodies to watch in 2017. MAbs. 9(2): 167–181.

Kazandjian D, Suzman DL, Blumenthal G, Mushti S, He K, Libeg M, Keegan P, Pazdur R. 2016. FDA Approval Summary: Nivolumab for the Treatment of Metastatic Non-Small Cell Lung Cancer With Progression On or After Platinum-Based Chemotherapy. Oncologist. 21(5):634-42

Kirkwood J, Butterfield L, Tarhini A, Zarour H, Kalinski P and Ferrone S. 2012. Immunotherapy of cancer in 2012. CA Cancer J Clin. 62(5):309–335.

Klapper LN, Kirschbaum MH, Sela M, Yarden Y. 2000. Biochemical and clinical implications of the ErbB/HER signaling network of growth factor receptors. Adv Cancer Res. 77:25-79.

Koebel CM, Vermi W, Swann JB, Zerafa N, Rodig SJ, Old LJ, Smyth MJ, Schreiber RD. 2007. Adaptive immunity maintains occult cancer in an equilibrium state. Nature. 450(7171):903-7.

Kraft S, Fernandez-Figueras MT, Richarz NA, Flaherty KT, Hoang MP. 2017. PDL1 expression in desmoplastic melanoma is associated with tumor aggressiveness and progression. J Am Acad Dermatol. 77(3):534-542.

Larkin J, Hodi FS, Wolchok JD. 2015. Combined Nivolumab and Ipilimumab or Monotherapy in Untreated Melanoma. N Engl J Med. 373:23-34.

Leach DR, Krummel MF, Allison JP. 1996. Enhancement of antitumor immunity by CTLA-4 blockade. Science. 271(5256):1734-6.

Lee CS, Cragg M, Glennie M, Johnson P. 2013. Novel antibodies targeting immune regulatory checkpoints for cancer therapy. Br J Clin Pharmacol. 76(2):233-47.

Lehmann BD, Bauer JA, Chen X, Sanders ME, Chakravarthy AB, Shyr Y, Pietenpol JA.2011. Identification of human triple-negative breast cancer subtypes and preclinical models for selection of targeted therapies. J Clin Invest. 121(7):2750-67.

LoBuglio AF, Wheeler RH, Trang J, Haynes A, Rogers K, Harvey EB, Sun L, Ghrayeb J, Khazaeli MB. 1989. Mouse/human chimeric monoclonal antibody in man: kinetics and immune response. Proc Natl Acad Sci U S A. 86(11):4220-4.

Lohrisch C, Piccart M. 2001. HER2/neu as a predictive factor in breast cancer. Clin Breast Cancer. 2(2):129-35.

Maçon-Lemaître L, Triebel F. 2005. The negative regulatory function of the lymphocyte-activation gene-3 co-receptor (CD223) on human T cells. Immunology. 115(2):170-8.

Mahoney KM, Rennert PD, Freeman GJ. 2015. Combination cancer immunotherapy and new Monica V. Goldberg, Charles G. Drake. 2011. LAG-3 in Cancer Immunotherapy. Curr Top Microbiol Immunol. 344: 269–278.

Massi D, Brusa D, Merelli B, Ciano M, Audrito V, Serra S, Buonincontri R, Baroni G, Nassini R, Minocci D, Cattaneo L, Tamborini E, Carobbio A, Rulli E, Deaglio S, Mandalà M. 2014. PD-L1 marks a subset of melanomas with
a shorter overall survival and distinct genetic and morphological chara cteristics. Ann Oncol. 25(12):2433-42.

Mitra D, Brumlik MJ, Okamgba SU, Zhu Y, Duplessis TT, Parvani JG, Lesko SM, Brogi E, Jones FE. 2009.
An oncogenic isoform of HER2 associated with locally disseminated breast cancer and trastuzumab resistance. Mol Cancer Ther. 8(8):2152-62.

Nahta R, Yu D, Hung MC, Hortobagyi GN, Esteva FJ. 2006. Mechanisms of disease: understanding resistance to HER2-targeted therapy in human breast cancer. Nat Clin Pract Oncol. 3(5):269-80.

Nagy P, Friedländer E, Tanner M, Kapanen AI, Carraway KL, Isola J, Jovin TM. 2005. Decreased accessibility and lack of activation of

ErbB2 in JIMT-1, a herceptin-resistant, MUC4-expressing breast cancer cell line. Cancer Res. 65(2):473-82.

Paciello R, Urbanowicz RA, Riccio G, Sasso E, McClure CP, Zambrano N, Ball JK, Cortese R, Nicosia A, De Lorenzo C. 2016. Novel human anti-claudin 1 mAbs inhibit hepatitis C virus infection and may synergize with anti-SRB1 mAb. J Gen Virol. 97(1):82-94.

Palmieri D, Richmond T, Piovan C, Sheetz T, Zanesi N, Troise F, James C, Wernicke D, Nyei F, Gordon TJ et al. 2015. Human anti-nucleolin recombinant immunoagent for cancer therapy. Proc Natl Acad Sci U S A. 112(30):9418-23.

Papaioannou NE, Beniata OV, Vitsos P, Tsitsilonis O, Samara P. 2016. Harnessing the immune system to improve cancer therapy. Ann Transl Med. 4(14):261.

Pardoll DM. 2012. The blockade of immune checkpoints in cancer immunotherapy. Nat Rev Cancer. 12(4):252-64.

Patel R, Bock M, Polotti CF, Elsamra S. 2017. Pharmacokinetic drug evaluation of atezolizumab for the treatment of locally advanced or metastatic urothelial carcinoma. Expert Opin Drug Metab Toxicol. 13(2):225-232.

Patel R, Bock M, Polotti CF, Elsamra S. 2017. Pharmacokinetic drug evaluation of atezolizumab for the treatment of locally advanced or metastatic urothelial carcinoma. Expert Opin Drug Metab Toxicol. 13(2):225-232.

Peggs KS, Quezada SA, Allison JP. 2009. Cancer immunotherapy: co-stimulatory agonists and co-inhibitory antagonists. Clin Exp Immunol. 157(1):9-19.

Raedler LA. 2015. Opdivo (Nivolumab): Second PD-1 Inhibitor Receives FDA Approval for Unresectable or Metastatic Melanoma. Am Health Drug Benefits. 8(Spec Feature):180-3.

Riccio G, Esposito G, Leoncini E, Contu R, Condorelli G, Chiariello M, Laccetti P, Hrelia S, D'Alessio G, De Lorenzo C. 2009. Cardiotoxic effects, or lack thereof, of anti-ErbB2 immunoagents. FASEB J. 23(9):3171-8.

Riccio G, Da Fonseca-Ricardo AR, Passariello M, Cunnah P, Mertens N, De Lorenzo C. 2017. Superior Suppression of ErbB2-positive Tumor Cells by a Novel Human Triparatopic Tribody. J Immunother. 40(4):117-128.

Robert C, Ribas A, Wolchok JD, Hodi FS, Hamid O, Kefford R, Weber JS, Joshua AM, Hwu WJ, Gangadhar TC et al. 2014. Anti-programmed-death-receptor-1 treatment with pembrolizumab in ipilimumab-refractory advanced melanoma: a randomised dose-comparison cohort of a phase 1 trial. Lancet. 384(9948):1109-17.

Romond EH, Perez EA, Bryant J, Suman VJ, Geyer CE Jr, Davidson NE, Tan-Chiu E, Martino S, Paik S, Kaufman PA et al. 2005. Trastuzumab plus adjuvant chemotherapy for operable HER2-positive breast cancer. N Engl J Med. 353(16):1673-84.

Sabatier R, Gonçalves A. 2014. [Pertuzumab (Perjeta®) approval in HER2-positive metastatic breast cancers]. Bull Cancer. 101(7-8):765-71.

Sanmamed MF, Pastor F, Rodriguez A, Perez-Gracia JL, Rodriguez-Ruiz ME, Jure-Kunkel M, Melero I. 2015. Agonists of Co-stimulation in Cancer Immunotherapy Directed Against CD137, OX40, GITR, CD27, CD28, and ICOS. Semin Oncol. 42(4):640-55.

Sasso E, D'Avino C, Passariello M, D'Alise AM, Siciliano D, Esposito ML, Froechlich G, Cortese R, Scarselli E, Zambrano N, Nicosia A, De Lorenzo C. 2018. Massive parallel screening of phage libraries for the generation of repertoires of human immunomodulatory monoclonal antibodies. MAbs. 10(7):1060-1072.

Sasso E, Paciello R, D'Auria F, Riccio G, Froechlich G, Cortese R, Nicosia A, De Lorenzo C, Zambrano N. 2015. One-Step Recovery of scFv Clones from High-Throughput Sequencing-Based Screening of Phage Display Libraries Challenged to Cells Expressing Native Claudin-1. Biomed Res Int. 2015:703213.

Savage P, Leventhal D and Malchow S. 2014. Shaping the repertoire of tumor-infiltrating effector and regulatory T cells. Immunol Rev. 259(1):245–258.

Scheuer W, Friess T, Burtscher H, Bossenmaier B, Endl J, Hasmann M. 2009. Strongly enhanced antitumor activity of trastuzumab and pertuzumab combination treatment on HER2-positive human xenograft tumor models. Cancer Res. 69(24):9330-6.

Seidman A, Hudis C, Pierri MK, Shak S, Paton V, Ashby M, Murphy M, Stewart SJ, Keefe D. 2002. Cardiac dysfunction in the trastuzumab clinical trials experience. J Clin Oncol. 20(5):1215-21.

Selby MJ, Engelhardt JJ, Johnston RJ, Lu LS, Han M, Thudium K, Yao D, Quigley M, Valle J, Wang C et al. 2016. Correction: Preclinical Development of Ipilimumab and Nivolumab Combination Immunotherapy: Mouse Tumor Models, In Vitro Functional Studies, and Cynomolgus Macaque Toxicology. PLoS One. 11(11):e0167251.

Shultz D. 2017. Three Drugs Approved for Urothelial Carcinoma by FDA. Cancer Discov.7(7):659-660.

Slamon DJ, Godolphin W, Jones LA, Holt JA, Wong SG, Keith DE, Levin WJ, Stuart SG, Udove J, Ullrich A et al.1989. Studies of the HER-2/neu proto-oncogene in human breast and ovarian cancer. Science. 244(4905):707-12.

Slamon DJ, Leyland-Jones B, Shak S, Fuchs H, Paton V, Bajamonde A, Fleming T, Eiermann W, Wolter J, Pegram M et al. 2001. Use of chemotherapy plus a monoclonal antibody against HER2 for metastatic breast cancer that overexpresses HER2. N Engl J Med. 344(11):783-92.

Stebbing J, Copson E, O'Reilly S. 2000. Herceptin (trastuzamab) in advanced breast cancer. Cancer Treat Rev. 26(4):287-90.

Steinman RM, Cohn ZA. 1973. Identification of a novel cell type in peripheral lymphoid organs of mice. I. Morphology, quantitation, tissue distribution. J Exp Med. 137(5):1142-62.

Stommel JM, Kimmelman AC, Ying H, Nabioullin R, Ponugoti AH, Wiedemeyer R, Stegh AH, Bradner JE, Ligon KL, Brennan C et al. 2007. Coactivation of receptor tyrosine kinases affects the response of tumor cells to targeted therapies. Science. 318(5848):287-90.

Stovgaard ES, Nielsen D, Hogdall E, Balslev E. 2018. Triple negative breast cancer - prognostic role of immune-related factors: a systematic review. Acta Oncol. 57(1):74-82.

Stuart BW and Kleiheus P. 2006. World Cancer Report-World Health Organization.

Tagliabue E, Centis F, Campiglio M, Mastroianni A, Martignone S, Pellegrini R, Casalini P, Lanzi C, Ménard S, Colnaghi MI. 1991. Selection of monoclonal antibodies which induce internalization and phosphorylation of p185HER2 and growth inhibition of cells with HER2/NEU gene amplification. Int J Cancer. 47(6):933-7.

Thorpe SJ, Turner C, Heath A, Feavers I, Vatn I, Natvig JB, Thompson KM. 2003. Clonal analysis of a human antimouse antibody (HAMA) response. Scand J Immunol. 57(1):85-92.

Troise F, Monti M, Merlino A, Cozzolino F, Fedele C, Russo Krauss I, Sica F, Pucci P, D'Alessio G, De Lorenzo C. 2011. A novel ErbB2 epitope targeted by human antitumor immunoagents. FEBS J. 278(7):1156-66.

Tuerk C, Gold L. 1990. Systematic evolution of ligands by exponential enrichment: RNA ligands to bacteriophage T4 DNA polymerase. Science. 249(4968):505-10.

Turcotte M, Allard D, Mittal D, Bareche Y, Buisseret L, José V, Pommey S, Delisle V, Loi S, Joensuu H et al. 2017. CD73 Promotes Resistance to HER2/ErbB2 Antibody Therapy. Cancer Res. 77(20):5652-5663.

Velcheti V, Schalper KA, Carvajal DE, Anagnostou VK, Syrigos KN, Sznol M, Herbst RS, Gettinger SN, Chen L, Rimm DL. 2014. Programmed death ligand-1 expression in non-small cell lung cancer. Lab Invest. 94(1):107-16.

Wang C, Thudium KB, Han M, Wang XT, Huang H, Feingersh D, Garcia C, Wu Y, Kuhne M, Srinivasan M et al. 2014. In vitro characterization of the anti-PD-1 antibody nivolumab, BMS-936558, and in vivo toxicology in non-human primates. Cancer Immunol Res. 2(9):846-56.

Wang S, Campos J, Gallotta M, Gong M, Crain C, Naik E, Coffman RL, Guiducci C. 2016. Intratumoral injection of a CpG oligonucleotide reverts resistance to PD-1 blockade by expanding multifunctional CD8+ T cells. Proc Natl Acad Sci U S A. 113(46):E7240-E7249.

Watanabe N, Gavrieli M, Sedy JR, Yang J, Fallarino F, Loftin SK, Hurchla MA, Zimmerman N, Sim J, Zang X, et al. BTLA is a lymphocyte inhibitory receptor with similarities to CTLA-4 and PD-1. Nat Immunol. 20034(7):670-9.

Wen T, Bukczynski J, Watts TH. 2002. 4-1BB ligand-mediated costimulation of human T cells induces CD4 and CD8 T cell expansion, cytokine production, and the development of cytolytic effector function. J Immunol. 168(10):4897-906.

Wimberly H, Brown JR, Schalper K, Haack H, Silver MR, Nixon C, Bossuyt V, Pusztai L, Lannin DR, Rimm DL. 2015. PD-L1 Expression Correlates with Tumor-Infiltrating Lymphocytes and Response to Neoadjuvant Chemotherapy in Breast Cancer. Cancer Immunol Res. 3(4):326-32.

Wurz GT, Kao CJ, DeGregorio MW. 2016. Novel cancer antigens for personalized immunotherapies: latest evidence and clinical potential. Ther Adv Med Oncol. 8(1):4-31.

Yarden Y, Sliwkowski MX. 2001. Untangling the ErbB signalling network. Nat Rev Mol Cell Biol. 2(2):127-37.

Zheng L, Tan W, Zhang J, Yuan D, Yang J, Liu H. 2014. Combining trastuzumab and cetuximab combats trastuzumab-resistant gastric cancer by effective inhibition of EGFR/ErbB2 heterodimerization and signaling. Cancer Immunol Immunother. 63(6):581-6.

LIST OF PUBBLICATIONS

Riccio G, Da Fonseca-Ricardo AR, **Passariello M**, Cunnah P, Mertens N, De Lorenzo C. 2017. Superior Suppression of ErbB2-positive Tumor Cells by a Novel Human Triparatopic Tribody. J Immunother. 40(4):117-128. doi: 10.1097/CJI.0000000000000152.

Sasso E, Latino D, Froechlich G, Succoio M, **Passariello M**, De Lorenzo C, Nicosia A, Zambrano N. 2018. A long non-coding SINEUP RNA boosts semi-stable production of fully human monoclonal antibodies in HEK293E cells. MAbs. 10(5):730-737. doi: 10.1080/19420862.2018.1463945.

Sasso E*, D'Avino C*, **Passariello M***, D'Alise AM, Siciliano D, Esposito ML, Froechlich G, Cortese R, Scarselli E, Zambrano N, Nicosia A, De Lorenzo C. 2018. Massive parallel screening of phage libraries for the generation of repertoires of human immunomodulatory monoclonal antibodies. MAbs. 10(7):1060-1072. doi: 10.1080/19420862.2018.1496772.

Riccio G, Ricardo AR, **Passariello M**, Saraiva K, Rubino V, Cunnah P, Mertens N, De Lorenzo C. 2019. T-cell Activating Tribodies as a Novel Approach for Efficient Killing of ErbB2-positive Cancer Cells. J Immunother. 42(1):1-10.doi: 10.1097/CJI.0000000000000248.